State University of New York at Stony Brook College of Engineering and Applied Sciences

Technical Report No. 740

The Role of Compact Nuclear Rockets in Expanding the Capability for Solar System Science and Exploration

James Powell, Department of Material Science
John Paniagua, Department of Mechanical Engineering
College of Engineering and Applied Sciences
State University of New York at Stony Brook
Stony Brook, NY 11794

George Maise
G. Maise Aeronautical Associates
Stony Brook, NY 11794

Hans Ludewig and Michael Todosow
Brookhaven National Laboratory
Upton, New York 11973

August 24, 1997

TABLE OF CONTENTS

EXECUTIVE SUMMARY

At present, solar system exploration is severely constrained by the inherent limitations of chemical rockets. Missions requiring high ΔV's are either not feasible or have to use very large and expensive launch vehicles. Trip times are many years, particularly for missions to the outer planets. These limitations arise from the inherently low specific impulse, I_{SP} (kilogram force sec of impulse per kilogram of propellant expended), of chemical fuels. The best chemical rockets known, i.e., hydrogen-oxygen, achieve an I_{SP} of about 450 seconds, with a corresponding practical limit on mission ΔV of only ~10 km/sec. No significant improvement in I_{SP} and mission ΔV appears possible using chemical rocket technology.

Very large improvements in I_{SP} and mission ΔV appear possible with nuclear rockets, however. Because the propellant, i.e., pure hydrogen, used in nuclear engines has a very low molecular weight, the I_{SP} is much higher, ~1000 seconds, with a much greater practical limit on mission ΔV, e.g., over 20 km/sec.

Nuclear engines can enable a quantum jump in the capability to carry out exploration of the solar system, particularly with regard to the more distant planets and moons. For the kinds of missions now being carried out, i.e., flybys, orbiters, and planetary probes, nuclear engines will result in much shorter trip times and much smaller and cheaper launch vehicles.

Moreover, nuclear engines not only offer large quantitative benefits for solar system exploration, but in addition, they make possible major new qualitative benefits. Missions that would yield important new scientific knowledge, but which are not feasible with chemical rockets, could be carried out with nuclear engines. Two very attractive possibilities are: 1) refueling with extraterrestrial propellant material, e.g., hydrogen derived from ice, to enable the return of samples from distant objects like moons (e.g., Europa), asteroids, comets, etc., and 2) virtually unlimited flight of instrumented probes in planetary atmospheres (e.g., Jupiter, Saturn, Uranus, Neptune, and moons such as Titan) using the atmosphere itself as the propellant.

A new ultra compact nuclear engine, MITEE (MIniature ReacTor EnginE), is described and its performance evaluated for various solar system exploration missions. The MITEE concept is based on the Particle Bed Reactor (PBR), with modifications that enable a smaller, lighter nuclear engine. A range of MITEE Engine designs is described. Representative design parameters for the baseline MITEE reactor are: 75 MW(th) power level, 1000 seconds I_{SP}, 100 kilogram mass, 10 MW/Liter fuel element power density, 39 cm core diameter/height, and a multiplication factor of 1.07. Total engine mass, including turbo pump assembly, nozzles, controls, and contingency, is estimated to be 200 kilograms.

Using the MITEE engine, ultra fast, lightweight solar system exploration missions are enabled. A range of such missions has been analyzed using the MULIMP spacecraft trajectory code, and are described. Examples include [trip times are from a LEO (Low Earth Orbit) start]:

1. 7 year flyby of Pluto

2. 13 year orbiter capture at Pluto

3. 2 year orbiter capture at Jupiter

4. 3 year orbiter capture at Saturn

All of the above missions involve direct trajectories, and do not require any planetary gravity assists. In contrast, the corresponding chemical rocket missions would take much longer, involve multiple gravity assists, and require considerably larger launch vehicles and greater IMLEO (Initial Mass in Low Earth Orbit). The MITEE Missions listed above require IMLEO's in the range of 2 to 4 metric tons, and can be carried out using either the new low cost LMLV vehicle (~25M $ launch cost) or a Delta rocket.

Moreover, the MITEE engine enables unique missions not feasible with chemical rockets. For example, a spacecraft using a MITEE engine could land on Europa, refuel with hydrogen derived from the water ice covering, and return to Earth. Total trip time for the mission would be approximately 5 years. Similar missions could be carried out to the asteroids and appropriate comets.

A second example of a unique mission capability is the delivery of a compact lightweight instrumented nuclear ramjet flyer into a planetary atmosphere. The flyer would cruise over the complete surface of the planet, taking real time data on local atmospheric conditions (temperature, pressure, composition, and velocity, spectral behavior, etc.), along with data on surface features (if present). The data would be transmitted to an orbiting satellite, which then would transmit it back to Earth. In turn, the path and points visited by the flyer would be controlled from Earth, so that important locations could be investigated and monitored over time, as appropriate.

The nuclear ramjet flyer would be based on a modified version of the MITEE reactor used in the MITEE nuclear engine. If would operate at substantially lower outlet temperature and power density, enabling a very long operating, life, i.e., years. The flyer would collect data from many thousands of locations during its operation, allowing extremely detailed mapping of atmospheric and surface (if present) conditions.

With the accompanying MITEE engine, a payload that contained the orbiter and the atmospheric flyer could reach its destination very quickly, i.e., Jupiter in 2 years or Saturn in 3 years, to begin gathering planetary atmospheric data. Such a payload could be launched using a low cost launch vehicle, e.g., Delta or LMLV.

Manned Mars missions utilizing the MITEE engine have also been investigated. The reduction in IMLEO achievable using MITEE are extremely large. Total IMLEO for a MITEE mission for Mars is only 375 metric tons [Sum of IMLEO for the Mars Transfer Vehicle (MTV), Mars Cargo Vehicle (MCV), and the return Earth Transfer Vehicle (ETV)], based on a 2016 AD

opposition type mission, with a transit time (go and return) of 270 days (80 days out, a 30 day stay, and 160 days return) and refueling with hydrogen propellant processed from ice on Phobos.

Using chemical propellant rockets, the IMLEO for just the Mars Transfer Vehicle alone is 1340 metric tons compared to 172 metric tons for the MITEE version. The total IMLEO (MTV + MCV + ETV) with chemical propellants would be far larger. Considering that the launch cost to LEO is on the order of 10 million dollars per ton, the savings in launch costs enabled by development of the MITEE engine would be enormous, i.e., tens of billions of dollars.

With MITEE, Manned Mars missions become economically and technically practical. With only chemical propulsion, not only is the cost of missions too great, but trip times become excessive for humans.

MITEE uses the same radial flow geometry as the PBR, with the annular fuel region positioned between cold and hot frits to form the completed fuel element. Like the PBR, the cold frit controls coolant flow, in order to match local power to flow. MITEE uses a lithium -7 hydride moderator and reflector, like the PBR, that is encased in beryllium containers and cooled by the incoming hydrogen propellant. The MITEE core consists of 37 fuel elements.

The new features of MITEE, compared to the PBR, are:

1. Composite cermet metal matrix perforated fuel sheets, rather than the packed bed of small diameter fuel particles.

2. Individual pressure tube elements, each with their own nozzle, instead of the common pressure vessel and nozzle used in the PBR.

These modifications, together with the lower power level (75 MW) and the lower power density (10 MW/Liter), enable a smaller, lighter reactor with enhanced operating life capability. The annular fuel element region consists of a multi-layered perforated metal sheet arrangement. The small fuel particles are incorporated in the metal sheets to form a composite cermet (volume fraction of 50%), with appropriately positioned through-holes for hydrogen coolant flow. The annular fuel region is composed of three-zones: an outer cooler zone using Be matrix sheets, a middle zone using Mo sheets, and an inner hot zone using tungsten (separated ^{184}W) sheets.

Detailed MCNP 3-D neutronic analyses have been carried out for a range of MITEE designs to evaluate the effect of core size, fuel element pitch to diameter ratio, and fuel type (^{235}U and ^{233}U) on the multiplication factor (k_{eff}). The analyses, which are described in the paper, indicate that satisfactory k_{eff} can be obtained for a ^{235}U fueled compact MITEE reactor with a mass of 100 kilograms.

Based on the initial studies, the MITEE concept appears very promising. It can enable much faster exploration missions to the outer plants, with much lower launch costs, and eliminates the need for complex, high risk planetary gravity assists. Moreover, it enables fundamentally new kinds

of missions that are not feasible with chemical rockets.

The development of a MITEE engine appears straightforward and affordable. Much of the development work has already been done in connection with the PBR program carried out in the late 1980's and early 1990's. Testing of a small nuclear engine (e.g., 75 MW) rather than the 1000 MW PBR will be much lower in cost, and more rapidly accomplished. A 3 phase MITEE development program is outlined, which would result in an operationally ready engine within 6 years from the date of start of the program. The cost to develop MITEE capability, projected to be on the order of 800 million dollars, is much less than the savings it would enable in launch costs for exploration missions based on chemical rockets. Moreover, it would yield additional benefits in terms of lower risk of failure, much shorter time to carry out missions, and the enablement of very attractive missions not feasible with chemical rockets. While it is not possible to quantify dollar savings for these benefits, they are real, and very important.

Nuclear rockets for long range solar system exploration are not hazardous. They would only start up in deep space, well away from the Earth. Until start up, nuclear rockets are not radioactive. In contrast, the radioisotope power sources (e.g., ^{238}Pu) on spacecraft currently being launched from Earth are highly radioactive. In the launch phase, safety systems would prevent reactor criticality for all conceivable accident situations until nuclear safe orbit was achieved. Finally, even after operation, the long lived radioactive inventory (e.g., ^{139}Cs and ^{90}Sr) would be negligible, typically about one-millionth of the radioactive inventory in a conventional earth based light water power reactor.

1. INTRODUCTION AND BACKGROUND

The inherent propulsive limitations of chemical rockets severely constrain solar system exploration. Many important missions are impossible, and the feasible ones are very expensive. The limitations result from the fixed amount of available chemical energy and the high molecular weight of the propellant reaction products, and cannot be overcome.

The propulsive performance of nuclear rockets is much greater than chemical rockets. In a nuclear thermal rocket fuel elements heat a low molecular weight propellant, typically pure hydrogen, to approximately 3000 K. At such temperatures, the specific impulse (kilograms force sec. of impulse per kg of expended propellant) of pure hydrogen is more than twice that of the best chemical propellant, hydrogen-oxygen.

The higher specific impulse enables a nuclear rocket to reach its destination in a much shorter time than a chemical rocket can, assuming the same payload. Also, the launch cost for the nuclear rocket will be much smaller since its launch mass is much less. Examples of this superior performance are given later.

Moreover, nuclear thermal rockets can use extraterrestrial resources as propellants, an option not practical with chemical rockets. This "refueling" capability would enable nuclear rockets to carry out very high ΔV missions, such as the return of large amounts of extraterrestrial material to Earth, and virtually unlimited flight in planetary atmospheres.

Nuclear rockets for long range solar system exploration are not hazardous. They would only start up in deep space, well away from the Earth. Until start up, nuclear rockets are not radioactive. In contrast, the radioisotope power sources (e.g., ^{238}Pu) on spacecraft currently being launched from Earth are highly radioactive. In the launch phase, safety systems would prevent reactor criticality for all conceivable accident situations until nuclear safe orbit was achieved. Finally, even after operation, the long lived radioactive inventory (e.g., ^{139}Cs and ^{90}Sr) would be negligible, typically about one-millionth of the radioactive inventory in a conventional earth based light water power reactor.

Development of nuclear rockets started in the 1950's in the US and USSR. Early versions were large and heavy, with low thrust to weight ratios (kg of thrust per kg of engine mass). More recent development efforts have been directed towards small, high thrust to weight ratio rockets. With some further development, a nuclear engine (i.e., reactor, pump, and control systems) weight of approximately 200 kg appears achievable, with a thrust to weight ratio in the range of 10 to 15. To date, nuclear rockets have only been ground tested, but there appears to be no reason why their in-flight performance should not be as predicted.

2. UNIQUE CAPABILITIES OF NUCLEAR ROCKETS

The specific impulse, I_{sp}, of a rocket is related to the exhaust velocity, V_{ex}, of the propellant leaving the nozzle by

$$I_{SP} = V_{ex}/g = \left(\eta_N\right)\frac{1}{g}\sqrt{\frac{2kR}{(k-1)}\frac{T_o}{M_W}}\ seconds \qquad (2.1)$$

where g is the Earth's gravitational acceleration (9.8 m/sec^2). The exhaust velocity (m/sec) is in turn determined by the propellant parameters - chamber temperature (T_o), molecular weight (M_W), and the ratio of specific heats ($k = C_P/C_V$), together with the nozzle expansion efficiency, η_N, which is typically close to 100%. R is the universal gas constant.

Since the chamber temperature for rockets is limited to ~ 3000 K by materials and coolability the primary factor determining I_{SP} is the molecular weight of the propellant. Nuclear rockets using pure hydrogen propellant ($M_W = 2$) can achieve an I_{SP} of ~1000 seconds. The I_{SP} for most solid and liquid fuel chemical rockets is only about 300 seconds, because of their much higher molecular weight propellants. The performance of hydrogen-oxygen chemical rockets is somewhat better, but the maximum I_{SP} is still only about 450 seconds.

For a single stage rocket leaving Earth orbit, the mass ratio (initial mass divided by final mass) is

$$\frac{m_o}{m_f} = \frac{m_p + m_T + m_{pay} + m_{eng}}{m_T + m_{pay} + m_{eng}} = \exp\left(\frac{\Delta V}{V_{ex}}\right) = \exp\left(\frac{\Delta V}{I_{SP}g}\right) \qquad (2.2)$$

where m_o is the initial total mass in low Earth orbit (IMLEO); m_f, the mass after the final burn; m_p, the propellant mass carried by the rocket; m_T, the tankage structure mass; m_{pay}, the payload mass; m_{eng}, the engine mass; and the total ΔV is the sum of the magnitudes of the velocity increments imparted by the individual sequential burns.

The tankage structural mass is expressed as a fraction, λ, of the total mass of the tank, including propellant; that is,

$$m_T = \lambda\left(m_P + m_T\right) \qquad (2.3)$$

Combining equations (2.2) and (2.3)

$$m_o = \frac{(1 - \lambda)\left[m_{pay} + m_{eng} \right] \exp\left(\Delta V / g I_{sp}\right)}{\left[1 - \lambda \exp\left(\Delta V / g I_{sp}\right) \right]} \qquad (2.4)$$

Figure 2.1 compares the initial mass, m_o, in orbit for nuclear thermal and chemical rockets, as a function of mission ΔV. The tankage mass fraction, λ, ranges from a lower bound of 0.05, corresponding to high strength composite tanks, to an upper bound of 0.10, corresponding to conservative aluminum tanks. The value of $\lambda = 0.05$ appears achievable.

The initial mass in low Earth orbit (IMLEO) for various solar system exploration missions is shown as a function of mission ΔV (sum of ΔV magnitudes in a multi-burn mission), engine type (chemical and nuclear thermal) and tankage fraction λ (fraction of loaded propellant tank devoted to structure). Single stage rockets are assumed (multi-stage performance is slightly better). Specific impulse is 1000 seconds for nuclear rockets and 450 seconds for chemical (hydrogen-oxygen) systems. Engine and payload mass total 500 kilograms. Practical limits for mission ΔV are ~10 km/sec for chemical rockets, and ~22 km/sec for non-refueled nuclear rockets. With extraterrestrial refueling of nuclear rockets, ΔV capability is virtually unlimited. The missions indicated are not possible using chemical rockets, but are practical with nuclear rockets using low cost Delta or LMLV launch systems.

Single stage H_2/O_2 chemical rockets have a practical limit of ~10 km/sec for mission ΔV, as determined by the limit of $m_o \rightarrow \infty$ as $\exp(\Delta V/gI_{sp}) \rightarrow \lambda^{-1}$. Multi-staging improves performance, but the increase in the ΔV limit is relatively small. Nuclear rockets, because of their much greater specific impulse, have a much higher practical limit for ΔV, ~22 km/sec.

Figure 2.1 shows the ΔV required for four missions that are only possible using nuclear rockets. These missions, and others, are discussed in detail later. Missions with ΔV requirements much greater than 22 km/sec are possible if the nuclear thermal rocket is refueled with extraterrestrial propellants - an option not practical for chemical rockets.

Figure 2.2 illustrates four types of unique missions only possible with nuclear engines. Type I missions involve high ΔV, direct trajectory, short trip time flyby or orbital capture missions to the outer planets or moons, using only propellant carried from Earth. Type II missions enable ultra long range flight of sensor platforms in planetary atmospheres, using nuclear ramjets. Type III missions process indigenous extraterrestrial materials (e.g., H_2O ice or methane) so as to refuel with hydrogen propellant. The increased ΔV capability enables the return of extraterrestrial samples to Earth, as well as longer range missions (e.g., asteriod hopping or distant comet rendezvous). Type IV missions shuttle payloads between surface and orbit using nuclear engines operating with indigenous propellants (e.g., CO_2 or H_2O on Mars, or H_2O on the moon). In Type I missions, high velocity nuclear rockets enable very short trip times - a few years to the outer planets (Jupiter and beyond) and their moons. Both flyby and orbital capture missions are practical. Direct trajectories would be used, eliminating the need for multiple planetary gravity assists. All propellant would be carried from Earth orbit without refueling.

Illustrative Type I missions are described in more detail later. As a comparative example, the "Pluto Express" mission presently proposed by JPL (1) would launch two flyby spacecraft to Pluto using two Delta rockets. The two spacecrafts (100 kg each) would take 12 years to reach Pluto requiring three gravity assists at Venus and one gravity assist at Jupiter. With nuclear engines and a single LMLV launch vehicle - one fourth of the cost of two Delta launches - two such spacecraft could reach Pluto in only six years on direct trajectories without gravity assists.

In Type II missions, nuclear engines would power ultra long duration flyers in the atmospheres of the outer planets (Jupiter, Saturn, Uranus, and Neptune) and their larger moons (Titan and Triton). The flyer probably would be a nuclear ramjet. The reactor powered rocket would be modified so that it would heat ram compressed atmospheric propellant (primarily hydrogen plus helium), rather than pure hydrogen. The propellant temperature for ramjet operation would be much lower than for the rocket, ~1500 K compared to ~3000 K, enabling the engine to operate for a much longer period, i.e., months instead of hours. The operating reactor power density would also be much less for the ramjet.

As the atmosphere flyer cruised along at high speed, i.e., at a Mach number on the order of 3, it would transmit measurements of local atmospheric conditions - composition, pressure, temperature, wind velocity, etc. - to a companion orbiter satellite, which would relay the information back to Earth. The flyer would provide data at many thousands of locations over the planet, yielding an extremely detailed 3D map of the planet's atmosphere. Flyers could monitor the time dependent behavior of important atmospheric regions, such as Jupiter's Great Red Spot, and highly turbulent equatorial region, or map surface relief features on its moons, such as Titan and Triton.

The flyer and its companion orbiter would be the payload for a Type I nuclear rockets and could be delivered to Jupiter in only two years, or Saturn in three years, as discussed later.

In Type III missions, the nuclear rocket would be refueled with hydrogen derived from suitable extraterrestrial materials, e.g., H_2O ice or methane, that are found on many bodies in the solar system. Total ΔV capability would then be well beyond the ~22 km/sec limit, enabling in a relatively short time the return of substantial amounts of extraterrestrial material from suitable moons, such as Europa, Phobos, and Titan; planets (e.g., Mars); icy asteroids; and comets.

Processing extraterrestrial materials for hydrogen propellant will require nuclear electric power sources based on reactors, since the output of radioisotope sources is far too small for practical missions. Typically, power outputs of tens of kilowatts would be required. Nuclear propulsion engines could be designed to operate bimodally, producing electric power when not thrusting. However, such technology appears very difficult and complex, and using a separate small nuclear power reactor would be much easier. Substantial development has already been carried out for a variety of nuclear electric systems, including closed Brayton cycles, thermionics and thermoelectrics. The processing unit could remain in place so as to provide return propellant for multiple missions.

In Type IV missions, the nuclear rocket would shuttle payloads between the surface of the planet or moon and an orbital station, reducing the ΔV requirements for journeys to and from Earth. Payloads to the surface would include personnel and supplies to Earth, while payloads to orbit could include personnel, extraterrestrial materials for return to Earth, along with hydrogen propellant derived from indigenous materials. Potential applications include a Mars shuttle, using as propellant either CO_2 from the atmosphere (2) or H_2O from the polar caps or Phobos, and a lunar shuttle, using H_2O from the poles (3). The lower ΔV requirements - a few km/sec - for shuttling would allow the direct use of CO_2 or H_2O as the propellant in the shuttle eliminating the need for processing to hydrogen.

Nuclear electric rockets also have been proposed for high ΔV missions (4). Potentially they have very high specific impulses, well above 1000 seconds, using electric energy generated by an on-board power reactor to accelerate the propellant in an ion engine or magnetic plasmadynamo-accelerator. Nuclear electric rockets, however, have very high specific masses, i.e., kg/kw(e). As a result, their acceleration capability is extremely small, and the trip times would be unacceptable for the types of missions considered here. However, nuclear electric rockets could play an important role as very long range probes, exploring interstellar space well beyond the limits of the Solar System.

3. STATUS OF NUCLEAR THERMAL PROPULSION

Nuclear Thermal Propulsion (NTP) engines have undergone extensive development in the United States (US), and in the Former Soviet Union (FSU). In the US, the NERVA system (5,6) was developed and successfully ground tested. The NERVA reactor consisted of many hexagonal-shaped fuel elements each of which contained fissile material and axial flow coolant channels (Figure 3.1A). Typically, the cores were about 1 m to 2 m in length, with length/diameter ratios of approximately unity. The reactors were graphite moderated, which was necessary since a large portion of the core operated at high temperature. Because graphite is a relatively poor moderator, the minimum diameter required for criticality was approximately 1 m. As a result, the reactor's power (and thrust) had to be high - otherwise the thrust/weight ratio would be impractically low (less than 1). The nominal power level for NERVA engines was 1000 MW, though reactors were tested with power levels of up to 5000 MW. Later designs included some hydrogenous material in an effort to reduce the critical size. This approach was not tested in a NERVA engine.

The FSU nuclear rocket was based on a somewhat different design approach (7). The reactor fuel elements utilized bundles of many twisted cross-shaped rods (Figure 3.1B). The bundles had an axial length of approximately 10 cm and were stacked lengthwise inside a ceramic tube with ceramic separators between bundles to form the final fuel element which had a total length in the range of 1 to 1.5 meters, depending on the reactor design power. The fuel elements were arranged in a hexagonal lattice, with each element surrounded by a moderator of ZrHx that operated at the reactor's inlet temperature fuel. Elements incorporating bundles of twisted fuel rods were successfully tested in the FSU, using flowing hydrogen coolant at temperatures above 3000 K for periods of approximately 1 hr. Full engine tests comparable to those carried out for NERVA were not performed.

Both of these nuclear rocket systems were inherently very heavy, which made them of limited utility for space application. Work on the US NERVA engine stopped in 1972, for lack of a defined mission. Work on the FSU engine continued until the early 90's, but it also lacked a clear mission. These engines typically weighed several tons, a consequence of their poor neutron moderating properties. To achieve criticality, the reactors had to be physically large and very heavy. A further limitation was their low thrust/weight ratio, which was at best only 5/1, compared to 50/1 for conventional chemical rocket engines. High thrust/weight ratios minimize burn times, enabling more efficient thrusting.

Their low thrust/weight ratio was a consequence of low power density in the reactor. If the power density is low, the amount of power - and thrust - available from a unit volume of the reactor is low, resulting in a low thrust/weight ratio. Fuel element power densities in the NERVA and FSU reactors were in the range of 3 to 5 MW/L, with the average reactor power density substantially less.

This low power density resulted from two design features. First, the heat transfer area per unit volume of fuel element was very small (approximately 5 to 10 cm^2/cm^3), due to the relatively large dimensions of the coolant passages. This low heat transfer area limited the total heat flux per unit volume, resulting in low power densities. Second, the hydrogen coolant flowed axially along

the NERVA and FSU fuel elements. Because of the long flow path, typically 1 m to 2 m, coolant flow velocities had to be relatively low to achieve an acceptable pressure drop. This also limited fuel element power density.

Finally, the NERVA and FSU engines had a long startup time (approximately 30 to 60 seconds), because of thermal stress limitations in the fuel elements. Chemical rocket engines typically start in a few seconds. Slow starts penalize performance, because propellant is not used efficiently, and gravity losses become important.

Recognizing these fundamental problems, the US DOD (Department of Defense) undertook a new development program, termed SNTP (Space Nuclear Thermal Propulsion) in the mid 1980's, with the objective of developing a compact, lightweight nuclear engine that had a thrust/weight ratio comparable to chemical rockets, and which could reach full power in a few seconds from a cold condition. The SNTP engine was based on the Particle Bed Reactor (PBR), a concept previously studied by Brookhaven National Laboratory (BNL) (8,9). Organizations involved in the SNTP program included Brookhaven National Laboratory, Sandia National Laboratory, Grumman Corporation, Babcock and Wilcox, Allied Signal, Hercules, and General Dynamics. The SNTP program continued until 1993, when the end of the cold war terminated the mission need for a compact, lightweight nuclear engine.

Program accomplishments (10,11) included the development of small nuclear fuel particles capable of operating at 3000 K in high pressure hydrogen for more than an hour, experimental demonstration of 30 MW/L power densities in a PBR fuel element under transient non-nuclear blowdown conditions, nuclear criticality tests of the PBR reactor, initial nuclear testing of prototype PBR fuel elements, development and manufacture of suitable hot and cold frits, and detailed engineering designs of the PBR nuclear engine. At the close of the program the next step was to be the nuclear testing of PBR fuel elements in a compact reactor assembly, followed by the ground testing of a prototype PBR nuclear engine.

To overcome the limitations of the NERVA and FSU engines, three new design approaches were adopted for the PBR. First, a hydrogenous moderator was used. This is necessary for small size and weight (compact fast spectrum reactors are also possible, in principle, but the safety problems associated with hydrogen coolant and fast startup effectively preclude this option). Lithium hydride (using isotopically separated ^{7}Li, a material which is in plentiful supply) was chosen for the moderator. Lithium hydride has a low density (0.8 gm/cm^3) and high temperature capability (approximately 1000 K). Most of the PBR core volume was occupied by the lithium hydride moderator, which was kept at low temperature by the incoming liquid hydrogen propellant. Neutronic tests of PBR critical assemblies verified that the small size PBR would operate as a critical reactor, and that the power distributions predicted by Monte Carlo analyses (10,11) as well as the other predicted reactor parameters (i.e., temperature coefficient, void coefficient, etc.) were correct.

Second, the heat transfer area in the PBR fuel element is greater by a factor of 10 than that in the NERVA and FSU elements. This enabled much greater power densities. The PBR fuel

element consists of an annular packed bed of small diameter fuel particles positioned between two porous tubes termed "frits" (Figure 3.1C). The fuel particles were directly cooled by hydrogen. The small diameter of the particles (typically 400 microns), resulted in a very high heat transfer area per unit volume of fuel element particle bed (approximately 100 cm^2/cm^3), enabling very high power densities. Transient blowdown experiments on hot PBR fuel elements (non-nuclear heated) demonstrated approximately 30 MW/L capability. Refractory carbide coated nuclear fuel particles were tested at temperatures up to 3000 K in hydrogen, and demonstrated the capability to withstand corrosion attack for periods well in excess of one hour.

Third, a radial flow path through the annular bed of packed fuel particles was adopted (Figure 3.1C), instead of the axial flow geometry used in the NERVA and FSU fuel elements. The much shorter path length (approximately 1 cm, compared to 100 cm for the NERVA and FSU fuel elements). enabled much greater coolant flow velocities, and correspondingly increased power densities. Local coolant flow rate was controlled by appropriate local adjustments in the effective porosity of the outer porous tube (cold frit), which accounted for the major portion of the total pressure drop through the fuel element. [The fuel bed and inner porous tube (hot frit) accounted for only a small portion of the total pressure drop.]

The locally varying porosity of the cold frit fully compensated for all of the axial and azimuthal variations in reactor power, enabling the hydrogen leaving the hot frit to be at the same temperature everywhere in the reactor. This maximized engine performance, since the mixed mean coolant outlet temperature then equaled the limit set by material properties. Thermal hydraulic experiments on prototype fuel elements demonstrated the ability to locally control coolant flow. In addition, they demonstrated the ability to operate with temperature gradients of approximately 3000 K/cm in the packed particle bed, and to withstand very rapid particle temperature changes during startup (approximately 10,000 K/sec). The capability to manufacture cold frits with the required porosity variation was also demonstrated, along with the capability to manufacture hot frits that could withstand 3000 K hydrogen.

After exiting the hot frit, the 3000 K hydrogen propellant flowed out through the cylindrical channel inside the hot frit. The diameter of the channel increased along its length in order to maintain a constant flow Mach number (design value of approximately 0.25), as illustrated in Figure 3.2. The PBR reactor assembly consisted of a hexagonal array of 19 or 37 fuel elements, depending on the power level and neutronic design. The hot coolant exiting from the elements then flowed into a common outlet plenum, which connected with the exhaust nozzle. The fuel element assembly and reflector elements were enclosed in a pressure vessel, which was integrally connected to the exhaust nozzle.

At the close of the SNTP program, all of the various neutronic, materials, and thermal hydraulic issues identified at program start were essentially resolved. The next step planned was to extensively test the PBR nuclear fuel elements under prototype conditions. If the SNTP program had been completed, the PBR nuclear engine (Figure 3.3) was anticipated to have the following capabilities:

1) ~ 800 kg total engine weight (including turbo-pump and controls)

2) ~ 1000 s specific impulse,

3) ~ 20,000 kg force of thrust (power = 1000 MW)

4) ~ thrust/weight ratio ≅40/1

5) 2 seconds startup time (cold to full power)

Although the PBR nuclear engine offers a major advance over the NERVA/FSU engines in terms of much lower weight, higher thrust/weight ratio, and fast startup, it still appears too heavy for the new generation of lightweight, high performance spacecraft now envisioned for solar system exploration.

The following sections of this report describe a modification of the PBR approach that enables a lower engine weight (e.g., approximately 200 kg), along with a more conservative (lower) operating power density (10 MW/L). This new concept, termed the MITEE (MIniature ReacTor EnginE) nuclear engine, would enable the much higher performance required for the various exploration missions described previously.

4. MITEE CONCEPTUAL DESIGN

4.1 Description of Concept

Figure 4.1.1 illustrates the basic MITEE concept. In contrast to the PBR, which utilized a single relatively large pressure vessel, the MITEE core consists of a set of hexagonal pressure tubes, each containing an outer shell of moderator and an inner cylindrical fuel element. The hydrogen coolant flows radially inward through each cylindrical fuel element, where the cold (~100 K) inlet hydrogen is heated to approximately 3000 K.

Unlike the PBR, where the fissile fuel was comprised of coated small individual fuel particles (~ 400 microns OD), in MITEE the fuel is present as fibers or particles imbedded in a metal matrix sheet. The cermet sheets form a multi-layered annular fuel element in which each sheet in the roll is perforated with optimally sized cooling holes. As in the PBR, there is a central hot gas channel inside the hot frit, along which the hot hydrogen flows to exit through an appropriately sized nozzle.

In contrast to the PBR, the MITEE hot gas channels do not exit into a common hot gas plenum and a single exhaust nozzle. Instead, each pressure tube has its own individual nozzle. as shown in Figure 4.1.2. The combined thrust from the assembly of nozzles provides the total engine thrust. This arrangement results in a simpler and lighter engine.

In an arrangement similar to the PBR assembly shown in Figure 3.2, the MITEE core has 37 elements, each being a pressure tube, arranged in a hexagonal pattern. The core is surrounded by one or two rows (depending on design) of reflector elements, which have the same pitch as the fuel elements, and contain the same moderating material as the core. The moderator in the MITEE engine is lithium-7 hydride held inside beryllium jackets. Hydrogen cools the moderator in the reflector before flowing into the core.

The fuel element has three zones:

1) An outer zone of a beryllium metal matrix composite, containing graphite fibers that are infiltrated with uranium carbide or oxide,

2) A middle zone of molybdenum metal matrix composite, containing uranium oxide (UO_2) particles, and

3) An inner zone of tungsten metal matrix (the tungsten will be enriched in ^{184}W to reduce parasitic neutron losses) composite containing uranium oxide (UO_2) particles.

The heat transfer area in the perforated metal matrix is controlled by the hole diameter and number of holes (Figure 4.1.3). Studies indicate that a perforation fraction of ~ 25% results in acceptable heat transfer performance. The gas flow holes through the sheets are located in a grid

pattern of slightly depressed channels formed in the sheets. When the sheets are layered together, the raised portions prevent closure of the holes in the sheets. Gas exiting through the holes in one sheet then flows to, and enters, the holes in the next sheet. This flow arrangement helps to mix the gas flow between sheets, and reduces the chances of thermal instabilities. The first sheet in the multi-layer stack will have smaller holes in order to distribute and match the hydrogen flow to local variations in the radial, axial, and azimuthal nuclear power production. In effect, it functions like the cold frit in the original PBR reactor.

4.2 Neutronic Design Analyses

The conceptual design of a nuclear reactor powered rocket involves a wide variety of analyses, including reactor physics, heat transfer, fluid dynamics, and stress. The reactor size is initially estimated based on input from systems analyses and mission requirements. This estimate is first checked for criticality. Any core that cannot go critical is not feasible and thus eliminated. Acceptable core designs are then optimized by iterating among the reactor physics, heat transfer fluid dynamics and stress analysis calculations. The resultant reactor design can then be integrated into an overall engine system design and startup transients analyzed.

The dimensions of the reactors considered here are based on a fuel element average power density of 10 MW/L and a total reactor power of 75 MW. The fissile material in the fuel element is either ^{235}U (enriched to 93%) or ^{233}U. In all cases the diameter of the core equals its height. The core consists of 37 hexagonal elements, reflected by either one or two rows of reflector elements of equal size. The only variable available to change the multiplication factor (k_{eff}) of the core is the element pitch/diameter ratio. Increasing the pitch/diameter ratio increases the amount of moderator in the core, thus softening the neutron energy spectrum. If the core is under moderated, increasing the pitch/diameter ratio increases the value of k_{eff} (and vice-versa). If the core is over moderated, increasing the pitch/diameter ratio will reduce the value of k_{eff} and vice-versa. This effect is illustrated in Figure 4.2.1. The fuel consists of tungsten, molybdenum, and beryllium cermet sheets, each containing a volume fraction of 50% UO_2. The sheets are layered together to form the annular fuel element. The beryllium also acts as a moderator within the fuel element. The core moderator and the reflector moderator consist of a lithium/beryllium composite. Two rows of reflector elements are included, resulting in a total of sixty one elements in the reactor. All the analyses were carried out using the Monte Carlo code MCNP (12). This code uses combinatorial geometry to represent the reactor, and a point-wise cross section representation. The MCNP analyses essentially make no simplifying assumptions with regards to reactor geometry and nuclear data. Results from the critical experiments carried out on small PBR reactor assemblies agreed very closely with predictions using the MCNP code.

The predicted reactor mass is also shown on Figure 4.2.1. It is seen that the mass increases with increasing pitch/diameter ratio, causing the thrust/weight ratio to decrease. If values of k_{eff} greater than 1.05 are acceptable, the highest thrust/weight ratio is achieved for a reactor with a core pitch/diameter ratio of 2. This design is somewhat under moderated, and the addition of hydrogen propellant during startup would increase the multiplication factor. The most stable reactor at startup would have a pitch/diameter ratio of 2.5, resulting in the reactivity being unaffected by the addition

of the hydrogen propellant. The issue of MITEE reactor stability during startup, and how it impacts the choice of pitch/diameter ratio, requires further detailed analysis of the transient effects during startup. However, based on transient start up analyses of the PBR, it appears possible to safely start a MITEE reactor even if it is initially under-moderated (10).

The dimensions for the series of ^{233}U and ^{235}U fueled reactor cores studied are shown in Table 4.2.1. In all cases the fuel consisted of 93% enriched uranium. Lithium-7 hydride/beryllium is assumed for the moderator and reflector with a power density of 10 MW/L is assumed in the end element region. The core consists of 37 fuel elements and is reflected by 24 elements reflector elements.

Table 4.2.1 Dimensions for Selected MITEE Reactor Configurations

Case	Pitch/Diameter	Pitch (cm)	Core OD (cm)	Fuel Thickness (cm)	Reactor OD (cm)
^{235}U Fueled Cases and 75 MW					
1	1.5	4.53	31.71	1.013	40.77
2	1.5	4.53	31.71	1.013	40.77
3	2.0	5.532	38.724	0.886	49.788
4	2.0	5.532	38.724	0.886	49.788
5	2.5	6.465	45.255	0.796	58.185
6	2.5	6.465	45.255	0.796	58.185
7	3.0	7.35	51.45	0.728	66.15
8	3.0	7.35	51.45	0.728	66.15
^{233}U Fueled Cases and 50 MW					
9	1.5	3.939	27.573	0.907	35.451
10	2.0	4.804	33.628	0.795	43.236
11	2.5	5.61	39.27	0.716	50.49
12	3.0	6.372	44.604	0.656	57.348

Multiplication factors and mass estimates for the core (fuel and moderator) and total reactor mass corresponding to the above cases are given in Table 4.2.2. (More detailed parametric results for the various configurations are given in Appendix A).

Table 4.2.2 Physics Results for Selected MITEE Reactor Configurations

Case	UO_2 content (%)	Multiplication Factor (k_{eff})	Core Mass (kg)	Total Mass (kg)
		^{235}U Fueled Cases and 75 MW Power		
1	50	0.896		----
2	30	0.823		-----
3	50	1.072	72.8	99.5
4	30	1.005	72.8	99.5
5	50	1.114	92.5	133.9
6	30	1.037	92.5	133.9
7	50	1.087	117.2	176.7
8	30	1.005	117.2	176.7
		^{233}U Fueled Cases and 50 MW Power		
9	30	0.854		-----
10	30	1.051	47.0	66.0
11	30	1.113	60.0	88.0
12	30	1.092	76.0	116.0

The above results show the clear advantage of using ^{233}U fueled reactor cores. Since ^{233}U has superior nuclear properties to ^{235}U, it enables smaller, tighter reactors to be critical. By operating the ^{233}U reactors at modestly increased power densities, the same power and thrust as the heavier ^{235}U fueled cores could be obtained, significantly increasing the thrust/weight ratio. Finally, the amount of UO_2 required in the cermet is seen to be lower in the case of the ^{233}U fueled cores. This is significant since demonstrating acceptable performance of the more highly loaded fuel under operating conditions will be more challenging. The availability and handling requirements for ^{233}U fuel in nuclear rocket applications would have to be evaluated. It has been used in civilian power reactors, so in principle, it appears to be a practical option.

4.3 Thermal Hydraulic Design Analyses

The fluid dynamic and heat transfer problems associated with nuclear rocket reactors are very different from those in other reactors. The coolant temperature range within the reactor is much larger than in commercial reactors, as well as other special purpose reactors. In a rocket reactor the coolant enters at approximately 30 K and leaves at 3000 K. Furthermore, almost all the enthalpy increase takes place while the coolant passes through the thin fueled part of the fuel element. This results in steep temperature gradients. However, because it is expected that convective heat transfer will be dominant in an operating reactor, the temperature gradient across individual plates within the fuel element will be negligibly small. The radial temperature profile through a fuel element will thus be a step-wise function, varying from the inlet temperature of a few hundred degrees to the outlet temperature of ~3000 K. As discussed below, a preliminary estimate of this temperature distribution is shown on Figure 4.3.2.

The primary objective of the thermal hydraulic design is to provide sufficient coolant flow through the core to keep its solid components safely below their melting temperatures. Given the rate of heat production in the core and the maximum exit temperature of the coolant, one can readily calculate the required coolant mass flow rate through reactor. Thus,

$$\mathring{m} = Q/[c_p (T_{out} - T_{in})] \qquad \textbf{(4.3.1)}$$

where Q is the rate of heat production in the core (e.g., 50 or 75 MW), C_p is the average specific heat of hydrogen, and T_{in} and T_{out} are the inlet and outlet temperatures of the hydrogen, respectively. Assuming a hydrogen inlet temperature of 100 K into the fuel region and an exit temperature of 3000 K, we calculate the coolant flow rates as:

$\mathring{m}$ = 1.1 kg/s for the 50 MW reactor

$\mathring{m}$ = 1.6 kg/s for the 75 MW reactor

If the total temperature of the rocket exhaust is 3000 K (as assumed above) the temperature of the solid reactor core (most probably where the flow exits the core) must necessarily be somewhat higher than 3000 K. The temperature difference between the solid core and the coolant flowing adjacent to it is called the "film drop." The latter varies locally as the coolant flows through the core. As was pointed out in Section 2, for maximum performance of the rocket, it is necessary to have the coolant exit the nozzle at the highest possible temperature. At the same time, the solid core must, obviously, be kept below its melting temperature. To attempt to satisfy these two constraints, a goal of the hydrodynamic design is to minimize the film drop.

To calculate the film drop, one must conduct a heat transfer analysis of the fuel elements. As described in Section 4.1, the MITEE fuel element is formed by rolling a perforated sheet into an annular shape (see Figure 4.1.3), which is held between two porous frits. For this analysis it was assumed that the lateral heat conduction in the sheet is large, i.e., the lateral temperature gradients in the "raised portions" of the sheet are negligible. Because of the complex flow passages through the fuel region, a detailed convective heat transfer analysis was not carried out at this stage of design. Instead, a conservative approach was adopted in which all of the convective heat transfer was assumed to take place on the cylindrical inner surfaces of the perforating holes. This assumption is reasonable because the flow velocity is highest inside the tubes and a new (and thin) boundary layer forms at the entrance of each of the tubes. Because of the high conductivity of the metallic fuel matrix, the wall temperature of the tube is essentially constant. The heat transfer problem is thus one of internal flow in short tubes with the tube wall at a constant temperature. A heat transfer correlation corresponding to these conditions is presented in Rohsenow, et al, (13). Table 7 in Chapter 7 of Rohsenow presents a correlation between the average Nusselt number in the tube and a nondimensional length of the tube x^+, for a range of Prandtl numbers. The nondimensional tube length is defined as $x^+ = (x/r)/(RePr)$. The geometry of the fuel sheet used for the analysis is illustrated in Figure 4.3.1. For this geometry the voidage is 37% and the open (flow) area is 23%.

The reactor design designated as Case 3 in Section 4.2 was analyzed using the above model.

The fuel thickness (0.886 cm) was assumed to be composed of a wrap of 35 layers. It was further assumed that hydrogen enters the fuel region at 100 K (note: hydrogen is heated from 30 K to 100 K in the moderator) and exits at 3000 K. Based on these boundary conditions, the calculated temperature variation in the fuel region of the core is shown in Figure 4.3.2. The most significant result seen in this figure is that the film drop at the exit of the core is about 40 deg C. Thus, for an effective chamber temperature of the propellant of 3000 K, the fuel element will experience a maximum temperature of 3040 K. This appears achievable.

Since the film drop has a small, but significant, effect on the performance of the rocket, a simple parametric analysis aimed at possibly reducing the film drop was conducted. It is apparent that the film drop varies inversely with the effectiveness of heat transfer process from the fuel to the coolant. The heat transfer process can be enhanced either by increasing the heat transfer coefficient or by increasing the heat transfer area per unit core volume. The latter effect can be achieved simply by scaling down the geometry of the flow passages. In other words, if we had geometrically similar sheets of fuel, but decreased their thickness, the heat transfer area per unit volume would be increased. In the example described previously the fuel was composed of 35 layers. The problem was re-analyzed, keeping the overall dimensions of the fuel region constant, but altering the thickness of the fuel sheets. The results are illustrated in Figure 4.3.3. Clearly, for minimizing the film drop, it is desirable to decrease fuel sheet thickness. The minimum thickness of the fuel sheet will probably be limited by mechanical considerations, rather than thermal hydraulics.

Since the heat transfer model is conservative, it appears likely that the actual film drops will be smaller than projected. Moreover, since the temperature of the fuel is so close to that of the hydrogen propellant at the hot side of the fuel element, it is very likely that a propellant outlet temperature in the range of 2750 to 3000 K (I_{SP} ~900 to 1000 seconds) can be achieved using the tungsten matrix fuel in the final third of the MITEE fuel element.

4.4 Reference Design Parameters

MITEE Engine Design

The MITEE engine point design will be based on a reactor fueled by ^{235}U, generating 75 MW of thermal power, and operating at an average power density of 10 MW/L in the fuel portion of the fuel element. The salient reactor parameters are given below:

Power [MW (th)]	75
Average power density in fuel region (MW/L)	10
Fuel Element Pitch (cm)	5.533
Fuel Element Pitch/Diameter	2.0
Number of Fuel Elements	37
Number of Reflector Elements	24 (one row)
Moderator Type	LiH/Be
Reflector Type	LiH/Be
Percentage UO_2 in Metal Matrix	50

Core Diameter (cm)	38.724
Reactor Diameter (core+reflector) (cm)	49.79

The components and the basis for their respective mass estimates to be included in the engine configuration are given below:

1) Reactor - Consists of thirty seven fuel elements arranged in a hexagonal pattern. Each element has a moderating zone and a zone containing fissile material. The moderator is a $^{7}LiH/Be$ composite, while the fissile zone consists of three cermet fuel layers. The innermost layer (hottest) is a $UO_2/^{184}W$ cermet, the next layer a UO_2/Mo cermet, and the outermost layer (coolest and closest to the moderator) a UO_2/Be cermet. Individual pressure tubes, made of Be/graphite composite, encase each of the fuel elements. A lower grid plate is made of carbon/carbon, into which individual nozzles are machined.

2) Turbo-pump Assembly - The Turbo-Pump Assembly (TPA) is driven by the outlet coolant from one of the outer fuel elements, acting as a topping cycle. The turbine exhaust then expands through a final nozzle, generating additional thrust. The impact of the TPA flow on specific impulse and engine thrust is thus minimized. A mass estimate for the TPA is made by scaling from the SNTP program, using published scaling relationships. At a fixed operating pressure, the mass of the TPA scales as the quantity (power or flow rate) to the 1.5 power. The turbine rotor is made of coated carbon/carbon, the shaft is beryllium, and the pump rotor is of aluminum. The TPA housing is manufactured of carbon/carbon (hot section) and aluminum (cold section). Low atomic number materials minimize heating from the gamma-ray flux that the unit will be exposed to during operation.

3) Propellant management system - The propellant management system (PMS) is based on the SNTP design. The PMS mass is directly proportional to reactor power, for the same operating temperature and pressure.

4) Thrust vector control - The thrust vector control (TVC) system for MITEE is less complex than that for SNTP. The TVC mass scales directly with output thrust.

5) Nozzle - The MITEE engine uses individual nozzles for each fuel element. The nozzles utilize a coated (TaC) carbon/carbon structure. The surface material immediately under the coating is graphite, since TaC coated onto graphite resists hydrogen attack better than TaC coated directly onto carbon/carbon. A mass estimate for the nozzles was made by first calculating the mass of a solid block of graphite large enough to cover the lower part of the reactor, and thick enough to allow an expansion ratio of 120:1. (This is the maximum possible expansion ratio for a fuel element pitch/diameter ratio of 2.) The thirty seven nozzle flow volumes were then subtracted from the block volume. The residual volume multiplied by the density of graphite then yielded the nozzle mass.

6) Instrumentation - The instrumentation package is not as complicated as that for the SNTP. There have been advances in the technology for space system.

7) Contingency - A 50% contingency was included in the mass estimate to cover design uncertainties and non-included components. The major component not included is the shielding system, since its mass will depend on mission requirements and system design. It is not possible to ascribe a specific value for its mass. Neutron shielding would be provided by a combination of distance and moderation/absorption in the liquid hydrogen propellant tankage. Gamma shielding would be provided by a combination of a high Z shadow shield and distance to the payload.

The mass budget for the MITEE engine is given in Table 4.4.1.

Table 4.4.1 - Engine mass breakdown

Component	Mass (kg)
Reactor	100
Turbo-pump Assembly	5
Propellant Management System	6.5
Thrust Vector Control	4.5
Nozzle	15
Instrumentation	5
Contingency	64
Total	200

The thrust of a rocket equals the product of mass flow rate (kg/s) and specific impulse (s); the mass flow rate equals the power (W) divided by the enthalpy rise (J/kg). In the above MITEE design the specific impulse is 1000 seconds and the flow rate approximately 1.6 kg/s, yielding a thrust of 1600 kgf. The engine thrust/weight ratio is then 8.0.

4.5 MITEE Development Requirements

The development of the MITEE engine would utilize the very extensive experience base accumulated by the United States and the Former Soviet Union (FSU). A substantial portion of the development required for MITEE has already been achieved in connection with the PBR (Particle Bed Reactor) program, which was carried out in the US during the late 1980's and early 1990's.

In particular, the PBR program.

1) Demonstrated very high power densities in non-nuclear test prototype fuel elements tested in the blowdown mode (~30 MW/Liter, three times the MITEE design value of 10 MW/Liter).

2) Developed very high temperature coated fuel particles and hot frits and demonstrated their ability to operate in 3000 K hydrogen for more than one hour.

3) Tested a "cold critical" PBR nuclear reactor. Detailed measurements of reactor performance were carried out including multiplication factor, three dimensional power distribution, temperature and moderator coefficients, etc., which exhibited excellent agreement with analytical predictions.

4) Fabricated and tested variable porosity cold frits suitable for locally controlling coolant flow to match 3D power distribution in the reactor.

5) Developed a detailed design for a 1000 MW PBR nuclear engine system, including reactor, pressure vessel, nozzle, turbo-pump, and controls. Performance parameters for the PBR engine system included: thrust of 22,000 kilograms, I_{SP} of 1000 seconds, weight of 800 kilograms, and startup time (cold to full power) of 5 seconds.

6) Developed a detailed design for a nuclear engine test facility at the Nevada Test Site and accompanying test plan. Ground testing of full-up PBR engines was planned, prior to operational testing.

The development of the MITEE engine will be significantly simpler, easier, and lower in cost than for the PBR, for the following reasons:

1) The MITEE fuel elements operate at a much lower power density than PBR fuel elements (10 MW/Liter compared to 30 MW/Liter). This greatly eases the thermal hydraulic design, and provides a much greater design margin.

2) The MITEE fuel form (composite metal matrix cermet sheets) is simpler to fabricate and would have greater resistance to hydrogen attack. It is mechanically more stable and easier to control the local fuel density. Unlike the packed bed of fuel particles in the PBR, there is no possibility of fuel settling which might affect local power density, or mechanically deform the confining frits.

3) The coolant flow path through the annular fuel zone in the fuel element is much more precisely and easily controlled in MITEE than in the PBR, so that all regions in the fuel zone can be evenly cooled. Moreover, the possibility of local "hot spots" will be greatly reduced by the excellent 2D lateral thermal conductivity in the metal matrix fuel sheets, and the elimination of any chance of local thermal instability due to changes in gas viscosity with temperature. (The latter concern is removed in MITEE by the mixing of coolant flow between the metal sheets.)

4) The startup time for MITEE can be much longer than the PBR (e.g., 20 seconds compared to 5 seconds) without compromising engine performance. The much longer startup time greatly eases demands on the reactor control system and permits

a smoother, more controlled temperature rise in the fuel zone.

5) The individual pressure tube nozzle arrangement in the MITEE design for each fuel element greatly simplifies reactor construction by eliminating the need for a large diameter, high strength pressure vessel, with an attached, separately cooled nozzle, which was used in the design of the PBR.

6) The much lower power level for MITEE (75 MW compared to 1000 MW for the PBR) greatly eases the testing requirements, both in terms of testing the complete reactor assembly, and also in testing individual fuel elements. Each of the 37 fuel elements in MITEE has a total thermal power of only 2 MW, compared to almost 30 MW for the PBR.

7) The thermal hydraulic performance of the MITEE fuel elements can be fully tested and validated in a non-nuclear mode, using electrical heating of the metal matrix fuel sheets to simulate the nuclear heating process. Nuclear testing of the final fuel element design would still need to be carried out to confirm and validate the design, but the long lead times and great expense of nuclear tests can be largely bypassed with MITEE. With the PBR, in contrast, it is not feasible to electrically heat the fuel elements to simulate nuclear heating.

8) The primary mission for the PBR was as a high performance second stage for existing first stage boosters, with nuclear startup before achieving orbit. As a result, extensive ground testing of the full-up nuclear engine was considered necessary to assure safety, reliability, and mission performance. The associated ground test facility was very costly and required a long lead time. Full containment and assured safety were very strong drivers in developing the facility.

   Since the MITEE engine would only startup in an already achieved high orbit, it appears possible to test its operation in space, rather than in a ground based facility. Moreover, since the fabrication cost of MITEE test units should be modest and the launch vehicle costs relatively low, it appears much more cost effective to test in space rather than build a new dedicated ground test facility. It should be no harder to acquire the appropriate data from a space based MITEE test than from a ground test. Such tests can probably be carried out more quickly than in a ground facility.

9) At the time of the PBR development program, the nuclear rocket test facilities in the FSU were not accessible for testing a US nuclear rocket design. The FSU had extensive facilities for nuclear testing of single and multiple fuel element assemblies under realistic operational conditions. With the end of the Cold War, these facilities are now available to the US and could be used in a cooperative program to develop a MITEE engine. Much of the nuclear testing and material development could be carried out using these facilities, at considerably lower cost than in the US.

With the above as background, a 6 year development program for MITEE has been examined. The program, would be divided into 3 phases, each 2 years in length.

1. Phase 1 - Component Development and Testing

2. Phase 2 - Component and Assembly Validation

3. Phase 3 - Operational Testing of MITEE Engines

At the completion of Phase 3, the MITEE engine would have been validated as mission ready, and could be incorporated into a variety of space exploration missions.

A substantial portion of the MITEE development program would be carried out cooperatively with Russia and other nations of the FSU, using their existing facilities. In particular, their efforts would probably be concentrated in the development of the metal matrix cermet fuel and other reactor materials (e.g., hot and cold frits, nozzles, moderator) and the nuclear testing of prototype fuel elements (single and multiple, as appropriate).

Phase 3 operational testing is based on testing 4 MITEE engines in high orbit. Two engines would be launched on each of two boosters (LMLV or Delta) to give the total of 4 engines. The engines would be tested sequentially, with information from previous tests used to help guide the test sequence on the next engine. The engines could be identical or modified somewhat to test different versions or different operational conditions. For example, one could test an engine at 2750 K outlet temperature (I_{SP} of 900 seconds) and a second engine at 3000 K outlet temperature (I_{SP} of 1000 seconds). Depending on test results, one could then decide on whether to limit MITEE operation to 2750 K for the first generation of missions, or go to 3000 K.

The 2 launch vehicles would be spaced-in-time approximately 9 months to a year apart so that results from the first 2 MITEE engine tests could be used, if desired, to modify the next 2 MITEE engines scheduled for testing.

The estimated total program cost is 800 million dollars, with the Phase 3 testing accounting for 50% of the total. These estimates are of course very rough, and would have to be developed in much more detail before starting a MITEE development program. However, the launch cost for Titan IV is approximately 400 million dollars. Other launch systems, while not quite as costly, are still very expensive. Thus, a few MITEE missions would more than pay for development cost by the ability to greatly reduce the cost of the launch vehicles needed to carry out the missions.

5. POTENTIAL MITEE MISSIONS

5.1 Pluto Missions

Pluto, the last planet of our solar system, remains the only planet not yet explored by unmanned spacecraft. Pluto's distance and its elliptical, inclined orbit requires large energy expenditures for successful encounters with this remote planet in a reasonable amount of time. The Jet Propulsion Laboratory (JPL) is currently developing a fast fly-by mission to Pluto and its moon, Charon. The Pluto Express (1), as presently named, is scheduled to be launched in March, 2001. Pluto's atmosphere, because of its elliptical orbit, is predicted to collapse from its current gaseous state to a liquid state in 2020-2025. This presents an opportunity to observe drastic atmospheric changes on a planetary scale that will not be available again for many years since the orbital period of Pluto is approximately 240 years.

The preferred flight path for a fast Pluto mission is the direct trajectory approach which results in shorter transit times and a relatively benign radiation environment with few maneuvers since there are no gravity assist flybys. However, for flight times under 10 years this requires an expensive Titan IV/Centaur class launch vehicle with an additional upper stage motor. The mission was originally designed to follow a direct trajectory to Pluto and Charon. In order to reduce launch costs, the two spacecraft are now planned to use four gravitational assists, three at Venus and one at Jupiter, to send them to Pluto. Due to the limitations of chemical propulsion systems for fast and low-cost missions, the JPL mission consists of two spacecraft (14), each approximately 100 kg, to be launched on two Molniya or Delta launch vehicles to arrive at Pluto in approximately 12 years. Both satellites will perform a fast fly-by of Pluto and will be separated by 3.2 days to allow for observation of both sides of each body.

The missions considered in this analysis are restricted to starting from LEO only after being placed in a stable orbit by a launch vehicle. This simplifies and eases the safety issues and mitigates political concerns. High propulsive efficiency of the MITEE engine yields the benefits of reduced transit time, and a smaller launch vehicle.

The missions analyzed fall into three categories. The first, category fast fly-by missions, involve only a single burn in LEO and are simple from the standpoint of vehicle configuration. The second category, fast orbital capture missions, require a second burn for orbit capture at the target planet. The third category, lander missions, require additional propellant (as compared to capture missions) for landing on the target planet. The MULIMP trajectory code (15) was used to calculate Initial Mass in LEO (IMLEO) for a range of various mission durations centered about the 2005 Earth departure opportunity, for the three mission categories. No gravitational assists were employed in the analyses.

IMLEO is plotted against transit time in Figure 5.1.1. For the fly-by missions, since there is only a single impulse addition in LEO, the single stage vehicle configuration consists of the MITEE engine system, a propellant tank, control avionics, and the two spacecraft payload (total of 200 kg). An engine Isp of 900 seconds and a tankage fraction of 5% are taken as the baseline

parameters for the analyses. [Nuclear thermal propulsion systems have an advantage over chemical propulsion systems because the use of a single propellant simplifies vehicle design.] As shown in Figure 5.1.1, a 7 year fast fly-by mission results in an IMLEO of approximately 1800 kg.

Because orbiter and lander missions must perform multiple burns, they require long-term storage of propellant (16). Since nuclear and solar propellant heating both would act to boil off this stored propellant, mitigation strategies include tank insulation, use of slush hydrogen and active refrigeration. IMLEO optimization studies resulted in a two-stage vehicle configuration. The system weight of the MITEE engine is estimated at 200 kg. Adding restart capability to the engine design would result in a heavier engine due to increased design margin requirements and decay heat removal capability. The decay heating rate after engine firing is sufficient for core meltdown if cooling flow is not provided. The required cooldown propellant is typically an appreciable fraction of the impulse propellant, and can amount to an extra propellant loading that would be greater than the MITEE engine system weight. For these reasons, for two-stage vehicle configurations, the first stage MITEE engine used for departure burn is jettisoned along with its propellant tank after Earth departs. This ensures that the Pluto capture propellant tank is full for the interplanetary coast and eliminates the issues of a partially full propellant tank. In addition, the first stage tank requires much less insulation than the second stage capture tank since it is operational for only a short period. As seen in Figure 5.1.1, a 12 year capture mission results in a spacecraft IMLEO of 4540 kg for a 200 kg orbiter spacecraft payload. For 13 and 14 year missions, the IMLEO decreases to 3985 and 3595 kg respectively.

Lander missions require greater propellant loading for the second impulse firing at target planet as compared to orbiter missions, because of the additional velocity change required for planet landing (17). For a 12 year Pluto lander mission, the spacecraft IMLEO is 5340 kg, an increase of 800 kg as compared to the orbiter mission. Extending the mission, respectively, to 14 and 16 years yields an IMLEO of 4100 and 3500 kg for a 200 kg spacecraft payload.

5.2 Solar System Missions

Unmanned exploration of the Solar System has been limited by the large energy requirements of interplanetary trajectories (18). Current mission strategies involve use of gravitational assists from intermediate planets to assist in achieving these high energy trajectories with restricted payload sizes. This section describes how the MITEE engine removes these limitations and enables unique and scientifically important missions that are not feasible with chemical propulsion systems.

Two classes of Solar System missions are considered. MITEE technology is assumed to be available for flight-ready hardware in the year 2005. Launch opportunities occur during this year for all of the planets. Both mission classes assume LEO start of the engine following an Earth-to-orbit launch of a booster. The first class considered was a high-energy capture mission, similar to the Pluto orbiter mission and the two-stage vehicle configuration discussed earlier, for the outer giant planets, Jupiter and Saturn. The payload consists of a 200 kg spacecraft orbiter and a 400 kg nuclear-powered ramjet that serves as an atmospheric-flying, data-gathering probe upon reentry.

The second class includes the lander/return missions where the vehicle lands on the planet surface, collects sample specimens, refuels indigenously, and then returns to Earth. The spacecraft payload is set at 200 kg. Europa, one of Jupiter's moons and having extensive portions of its surface covered with hydrogen and Pluto have been selected for this mission class. Because more than two engine firings are required for this second type of mission, vehicle configuration optimization studies indicate that a lower IMLEO results from incorporating restart capability into a single-stage engine design with one main propellant tank. To account for decay heat cooldown propellant requirement, the tankage fraction is increased by an additional 5%.

Table 5.2.1 tabulates results for these missions. The IMLEO for a two-year orbiter mission to Jupiter and a three-year orbiter mission to Saturn are 3395 and 4170 kg, respectively. For comparison, Galileo requires 6 years (19) to reach Jupiter (which includes one Venus and two Earth gravity assists) and the Cassini mission to Saturn (20), as currently planned, requires 7 years to arrive. The Europa lander/return sample mission has a two year outbound direct trajectory with a 30 day stay on the satellite and culminates with a three year return after departure from Europa with the samples onboard. The IMLEO for this mission is 4610 kg.

An even more exotic mission is the Pluto lander/return sample mission. Because of the enormous distances involved, in order to limit the mission duration to less than 25 years, mission analysis required an increase in the baseline engine Isp to 1000 sec. The outbound flight will take approximately 12 years and is followed by a 30 day stay on the planet for indigenous refueling and sample collecting. The return flight to Earth will also last 12 years with termination of the mission in the year 2029. This results in an IMLEO of 9050 kg (Table 5.2.2).

5.3 Launch Vehicles for Outer Planet Missions

The Titan IV (21) is the nation's largest expendable launch vehicle and consists of two solid propellant stage motors, a liquid propellant two-stage core, and a 16.7-foot diameter payload fairing. The system can fly with a Centaur upper stage, an Inertial Upper Stage (IUS), or no upper stage. Overall length of the launch vehicle is 204 feet when flown with an 86-foot long payload fairing. The Titan IV Centaur is capable of placing 10,000-pound payloads into geosynchronous orbit, or 39,000 pounds into low-Earth orbit. The addition of upgraded solid rocket motors in 1996 as part of the Titan IV B enhanced configuration will enhance performance by approximately 25 percent. Launch costs are approximately $250-350 million.

The Atlas IIAS (21) is the fourth and most powerful variant in the Atlas family, with a payload lift capability in the 7,000 to 8,000-pound class range to geosynchronous transfer orbit. Four strap-on solid rocket motors been added to the booster to increase liftoff thrust and payload lift capability. The IIAS Centaur upper stage is powered by two Pratt & Whitney RL10 turbo pump-fed engines burning liquid oxygen and liquid hydrogen. The length of the launch vehicle with the large payload fairing is 156 ft. Launch costs are approximately $100 million.

The Delta II (21) is a medium capacity expendable launch vehicle built by McDonnell Douglas that can lift payloads up to 4,120 pounds to geosynchronous transfer orbit. Launch costs

are approximately $50 million. The Delta III is the newest and most powerful version of the Delta family of expendable launch vehicles slated for first launch in 1998. The Delta III will provide a payload lift capability of 18,400 pounds to low-Earth orbit and 8,400 pounds to geosynchronous transfer orbit which is twice the payload of the Delta II rocket. Compared to the Delta II, the Delta III's most notable changes include a larger composite fairing enlarged from 9.5 feet in diameter to 13.1 feet, larger and more powerful strap-on solid rocket motors, and a new cryogenically propelled single-engine upper stage.

The LMLV (21) is a low-cost series of small to medium launch vehicles developed through internal funds by Lockheed Martin. Through combinations of common components, an increasing payload lift capability from 800 to 3655 kg is achieved to low-Earth orbit. To minimize development cost and risk, the launch vehicles makes use of existing rocket motor designs and other elements. Launch costs are approximately $23-27 million.

The launch vehicle selection parameter is dictated not by its payload-lifting capability, but by the payload fairing volume of the booster. This is due to the nature of nuclear thermal propulsion (NTP) systems which utilize low density hydrogen propellant exclusively. NTP vehicles require five times the tank volume of chemical systems for the same propellant loading, resulting in decreased mass efficiency (22). Use of slush hydrogen would increase the propellant loading per unit volume of tankage.

The Pluto 7-year direct fast-flyby mission can be housed in a single Delta II or LMLV-3 payload fairing (Figure 5.3.1). For comparison, the current Pluto Express is slated to be launched on two Molniya or Delta vehicles scheduled to arrive at Pluto in 12 years after a series of gravitational assists. For the remaining missions discussed earlier a listing of the launch vehicles that can be used include:

- Atlas IIAS booster for the 13/14 year Pluto orbiter missions and 14/18 year Pluto lander missions
- Delta II or LMLV-3 launcher for a 16 year Pluto orbiter mission and 2 year Jupiter orbiter mission
- Atlas IIAS launcher for Saturn orbiter and Europa lander/sample return missions
- Pluto lander/sample return mission necessitates use of the Titan IV heavy-lift launcher due to the 100 m^3 propellant loading volume required by the spacecraft

Note this analysis did not utilize gravitational assists of intermediate planets which would reduce the spacecraft IMLEO.

The performance gains described in the mission analyses illustrate the enormous potential of the MITEE engine. The above benefits include the substantially reduced launch costs that are achieved through utilization of existing small-to-medium lift boosters, and the large performance increases in mission ΔV. These features will greatly expand our ability to explore the Solar System in both conventional and innovative missions.

5.4 Manned Mars Mission

In 1989, President Bush and the National Space Council identified the manned exploration of Mars as a major milestone in Man's conquest of space. Among the challenges and risks the undertaking poses include the enormous distance that has to be traversed. Traveling such a distance would take many months if current technology was applied, thereby increasing risk to both the crew and mission. NASA and industry recognize that the need for rapid transits can be satisfied by utilizing Nuclear Thermal Propulsion (NTP). These short transits offer important advantages to the crew, such as less exposure to cosmic radiation and zero-gravity. The Stafford Synthesis group has identified NTP as the propulsion system of choice for all manned Mars missions and for Lunar exploration (23).

The goal of achieving short transit times must be moderated by other considerations which include minimizing cost and risk. Cost can be controlled by minimizing IMLEO to an acceptable level. Other cost/risk reducing measures include minimizing the number of new development programs and complexity. This section discusses the benefits offered by a nuclear thermal rocket based on the MITEE engine for manned exploration of Mars. Specifically, the small engine enables short mission durations with round-trip transits on the order of 270 days centered about the 2016 Earth-Mars opposition.

Potential missions to Mars fall into two categories based on planetary positioning. Opposition class missions center about a Sun-Earth-Mars opposition where the Sun and Mars appear on opposite sides of the Earth. Conjunction class missions center about a Sun-Earth-Mars conjunction where the Sun and Mars appear on the same side of the Earth. Both classes of missions involve Mars arrival and departure at or near the opposition date. Opposition class missions, since they are centered about the same opposition, arrive and depart Mars during the same opposition. This limits the stay time on Mars to a few days or weeks since longer stays move arrival and departure further from the opposition date and end up requiring more energy. Conjunction class missions perform Earth-Mars transit about one opposition and perform Mars-Earth transit about the subsequent opposition. Since the synodic cycle, or time between oppositions, is about 26 months, conjunction class missions have long stay times, on the order of 2 years. The NASA 90 Day Study (24) identified opposition class missions as the most likely candidates for the initial exploration of Mars, and conjunction class missions as likely candidates for permanent colonization/base support.

The Martian orbit is fairly elliptical with an eccentricity of 9.3%, whereas the Earth's orbit is nearly perfectly circular. This results in substantial energy differences required for transfer orbits since Martian aphelion is 1.2 times its perihelion. Transfers occurring near Mars aphelion require significantly greater energy. It is apparent that some years are more favorable for launch opportunities than others. The NASA 90 Day Study planned its mission architecture for the easier 2016-2022 opportunities.

The ground rules for this analysis are based on the 90 Day Study and the results of previous

work (25). As noted, a "split/sprint" mission was utilized and seeks to minimize both crew transit time and IMLEO by delivering cargoes to Mars not required before Mars orbit on an unmanned vehicle traveling along a minimum energy trajectory. Concerns about crew welfare do not apply since the cargo vehicle is unmanned. The Mars Cargo Vehicle (MCV) includes the lander and ascent stage, all surface equipment, and the return Earth Transfer Vehicle (ETV). The crew travels to Mars on a Mars Transfer Vehicle (MTV) along a high energy trajectory and then completes a rendezvous with the MCV in Mars orbit. The crew habitat is then transferred to the ETV and the mission proceeds.

The 90 Day Study identified the year 2016 for the first manned exploration mission. This mission was classified as opposition class with a 30 day stay. This does not require an overly ambitious schedule and has a suitable stay time for a first trip. It also occurs during a moderately easy opportunity which is followed by several easier opportunities which makes a multi-missioning effort simpler. This analysis kept these ground rules for its reference mission.

Initial studies by Venetoklis et al. (25) found that fast all-propulsive missions were possible, so aerocapture and Apollo-type crew Earth reentry were not considered. Elimination of these two design features reduces high cost and risk development programs in addition to single-point failure modes. Also, maximum-speed restrictions at Mars and Earth capture imposed by physiological and technology limits are lifted. As a result, this enables faster transits. Mission ground rules and parameters are summarized in Table 5.4.1.

Figure 5.4.1 illustrates the crew vehicle configuration developed for this analysis. Two of these vehicles are required for the mission. One is for crew delivery to Mars (MTV), whereas the other is utilized for crew return to Earth (ETV). The long truss design is for reducing the radiation dosage to the crew. The ETV is brought to Mars orbit without the crew habitat by the cargo vehicle, MCV. The habitat is transferred from the MTV to the ETV in Mars orbit. The 25 metric ton habitat mass was derived in part from the approximate 28 metric ton value quoted in the NASA 90 Day Study. The 90 Day Study habitat has design features not required in the reference mission and is downsized accordingly. The ETV utilizes heavier insulated propellant tanks than the MTV due to greater idle mission time. Initial vehicle trade studies (26) indicated that advantages to staging are realized when using more than one propellant tank per vehicle. Four tanks are emptied for Earth departure and two tanks are used for Mars capture. The tanks can be filled with slush hydrogen to alleviate the boiloff problem. Tank placement is made with consideration for both center-of-gravity and engine radiation, and the engine shields were designed to protect the propellant tanks. The MCV is essentially similar and does not require a long truss since the vehicle is unmanned.

The initial goal of the study was to determine IMLEO reductions offered by the MITEE engine when applied to the NASA 90 Day Study reference mission and the work of Venetoklis, (25). The realization of the hazards of prolonged crew exposure to deep space shifted the focus away from IMLEO to short transit times. However, some guideline is needed to avoid developing an absurd design. Cost is the most obvious choice with IMLEO being its simple measure. An upper limit to IMLEO serves as a fence for limiting the efforts to shorten the trip. An upper limit of 1,000 metric tons was chosen for total IMLEO (MTV+MCV+ETV) for this mission. The MCV departs 870 days

prior to the MTV launch window opening during the previous opposition, permitting check-out of the lander and ETV prior to crew departure.

With the upper limit established, a minimum transit time was determined from utilizing in conjunction the MULIMP interplanetary trajectory optimization program. A 270 day opposition class mission was developed for the 2016 opportunity that met criteria and ground rules established before. Figure 5.4.2 illustrates the impact of transit times on the masses of the MTV and ETV for engine I_{SP}'s of 900 and 1,000 seconds. The tankage fraction is fixed at 10% with a 25 metric ton habitat payload. The tankage fraction assumption includes an "advanced technology" 5% tankage factor and additional reserves. For each stage, 5 MITEE engines are clustered to reduce the engine operating times for the firings. After each burn, the engine stages are discarded thereby eliminating the need for additional cooldown propellant. For the MTV, a 70 day outbound trip requires a 251 metric ton IMLEO. After a 30 day stay on the planet surface, a 170 day return trip requires an ETV mass of 128 metric tons with for a 25 metric ton habitat payload. The Mars cargo vehicle, MCV, which transported as its payload the lander and the ETV (minus the habitat) 870 days earlier is sized at 388 metric tons IMLEO. This brings total IMLEO to 639 metric tons. The burn time for the clustered engines at Earth orbit departure is over 10,000 seconds in this case. This requires a long engine operating life.

If the outbound journey is lengthened by 10 days and the return leg is shortened by the same amount to maintain the total mission time to 270 days, the MTV IMLEO is reduced to 172 metric tons, whereas the MCV IMLEO and ETV mass are increased to 482 and 172 metric tons, respectively. Total IMLEO is increased to 654 metric tons. Engine burn time at Earth orbit departure is decreased to 6,400 seconds, a much less stringent operating life. For this reason, this mission is selected as the baseline reference opposition class mission. Further increasing the outbound leg by 10 days to a transit time of 70 days results in an MTV IMLEO of approximately 131 metric tons. However, since the inbound leg duration has been decreased by the same amount to a transit time of 150 days, this results in a more energetic return transit which increases the ETV mass to 425 metric tons. The MCV IMLEO increases accordingly to over 1,000 metric tons. One note, however, is that the engine operating life is based on the assumption that there is no engine out scenario during the firing times. If there is a loss of engine, the engine burn times are increased accordingly and must be taken into account when comparing against the maximum engine operating life. Table 5.4.2 summarizes the opposition class mission analysis results.

The compact design of the MITEE propulsion system offers advantages over other nuclear rocket designs when incorporated into a high energy mission architecture. IMLEO is reduced due to the MITEE engine's small size and the elimination of the decay heat removal cooldown propellant requirement. When compared to a chemical-based cryogenic all-propulsive vehicle, the IMLEO alone for an MTV 80 day transit trip to Mars increases eight-fold to 1,340 metric tons. The energetic opposition class mission produces an excessive IMLEO for a cryogenic/all-propulsive vehicle. The NASA 90 Day Study defined a vehicle that was based on the cryogenic aerobrake concept. Use of aerobraking for capture at Mars and at Earth upon return reduces the IMLEO and allows use of cryogenic propulsion to accomplish the opposition class mission. However, the total mission time increases to 434 days and requires an inbound Venus swing by gravitational assist.

Total IMLEO for the cryogenic aerobrake vehicle is 828 metric tons (25), an increase of over 25%. As a final comparison, the same 270 day Mars opposition class mission utilizing a Particle Bed Reactor (25) increases the IMLEO by approximately 33%.

Further reductions in IMLEO can be achieved by refueling indigenously at the Martian satellites, Phobos and Deimos. Because the MCV does not have to haul the propellant for the ETV to Mars, its IMLEO decreases substantially by approximately 58% to 201 metric tons. Therefore, the total IMLEO reduces by 43% to 375 metric tons.

6. CONCLUSIONS

Solar system science and exploration mission capabilities would be dramatically enhanced by the development and utilization of a compact lightweight nuclear engine.

For missions to Jupiter and beyond, trip times could be shortened by at least a factor of 2. Moreover, direct trajectories would be used instead of the multiple planetary gravity assist missions now customary, enhancing reliability and reducing mission risk. In addition the size and cost of the launch vehicles required for the mission could be greatly reduced.

As examples of these capabilities, a small nuclear engine could put an orbiter around Jupiter in just 2 years, an orbiter around Saturn in 3, and an orbiter around Pluto in only 12 years, using small, low cost, readily available launch vehicles.

In addition to carrying out science and exploration missions faster and cheaper, compact nuclear engines can enable missions not feasible with chemical rockets. A very attractive example is to use a nuclear engine (e.g., a nuclear ramjet) to fly instrumented vehicles in planetary atmospheres (e.g., Jupiter, Saturn, Uranus, Neptune and Titan) for virtually unlimited periods, gathering an enormous amount of data on planetary atmospheric composition and behavior.

A second very attractive example of the unique capability of nuclear engines is to refuel with indigenous extra-terrestrial propellants (e.g., hydrogen derived from water ice) to enable sample return missions from Europa and other moons, asteroids, comets, etc.

Over the years there has been extensive development efforts on nuclear rockets in the US and FSU (Former Soviet Union). While nuclear rockets have not been flown as yet, much of the required development work has been carried out.

Earlier efforts were aimed at relatively heavy, low/thrust weight nuclear engines, such as the NERVA systems. Later efforts in the US in the late 80's and early 90's focused on the light weight Particle Bed Reactor (PBR) nuclear engine.

The PBR underwent substantial development, with the aim of achieving a 1000 MW, 500 kg nuclear engine capable of 1000 seconds specific impulse, a thrust of 22,000 kilograms and a thrust to weight ratio of 40/1.

Although the end of the Cold War resulted in the ending of the effort on the PBR nuclear rocket, program results indicated that the desired performance could be achieved.

Based on the PBR development results, a smaller, lighter modification appears practical, termed MITEE (MInature ReacTor EnginE). The MITEE engine is designed for lower power and lower power density than the PBR and could be developed for application in a relatively short time, e.g., 6 years.

The MITEE engine would have a power of 75 MW, power density of 10 MW/L in the fuel elements, and an I_{SP} of ~1000 seconds. Total engine weight, including reactor nozzles, turbo-pump, controls, etc. is projected to be only 200 kg, including a 30% contingency.

The development cost for MITEE is projected to be approximately 800 million dollars, based on nuclear testing of the fuel elements in existing FSU facilities, and tests of the final engine in space.

The development of MITEE would enable much faster, cheaper science missions, many of which would be of great scientific value, and which could never be carried out using chemical rockets. Moreover, development of the MITEE engine would also enable much faster, safer, and lower cost manned missions to Mars.

7. REFERENCES

1. "Ice and Fire Preprojects mission .... to explore Pluto/Charon", http://www.jpl.nasa.gov/pluto.

2. Zubrin, R., "Indigenous Martian Propellant," Aerospace America, p. 48, August, 1989.

3. Zuppero, A., personal communication, 1997.

4. Walter, C., "Gas-Cooled Reactor Power Systems for Space." Trans. 4th Symp. On Space Nuclear Power Systems, p. 419-422, Albuquerque, NM, 1987.

5. Durham, F.P., "Nuclear Engine Definition Study Preliminary Report," Vol. 1. Engine Description, Low Alamos Scientific Laboratory Informal Report, Los Alamos, NM, LA-5044-MS, Sept. 1972.

6. Koenig, D.R., "Experience Gained From the Space Nuclear Rocket Program," (Rover), Los Alamos Laboratory, Los Alamos, NM, LA-10062-H, May 1986.

7. Goldin, A.Y., et al., "Development of Nuclear Rocket Engines in the USSR," (presented by J.R. Wetch) AAIA Paper 191-3648, AIAA/NASA/OAI Conf. On Adv. SEI Technologies, Cleveland, Ohio, Sept. 1991.

8. Powell, J.R., et al., "High Power Density Reactors Based on Particle Bed Cooling,", Proc. 2nd Symp. on Space Nuclear Power Systems, Albq., NM, 1985.

9. Powell, J.R., "Particle Bed Reactor Orbit Transfer Vehicle," p. 221, BNL 40497, 1988.

10. Ludewig, H., et al., "Summary of Particle Bed Reactor Designs for the Space Nuclear Thermal Propulsion Program," BNL-52408, Sept. 1993.

11. Ludewig, H., et al., "Design of Particle Bed Reactors for the Space Nuclear Thermal Propulsion Program," Prog. in Nuc. Eng., 30, No. 1, p. 1-65, 1996.

12. Breismeister, J.F., "MCNP, A General Monte Carlo Code for Neutron and Photon Transport" (1986), Version 3A, LA7396-MS, Rev. 2, Los Alamos National Laboratory, Los Alamos, NM.

13. Rohsenow, W.M., et al., (Eds.), *Handbook of Heat Transfer Fundamentals*, McGraw-Hill Book Company, New York, 1985.

14. Price, H.W., et al., "Pluto Express Science craft System Design", IAA-L-0603, Jet Propulsion Lab, California Institute of Technology, http://www.jpl.nasa.gov/pluto/iaa_1.htm.

15. Friedlander, A., et al., "MULIMP Software Presentation and Demonstration", Science Applications International Corporation presentation to NASA MSFC, 15 December, 1988.

16. Venetoklis, P.S., Nelson, C., "Pluto Exploration Strategies Enabled by SNTP Technology", AIAA 93-1951, AIAA/NASA/OAI Conf. on Adv. SEI Technologies, Cleveland, Ohio, June, 1993.

17. Hale, F.J., Introduction to Spaceflight, New Jersey, Prentice Hall Inc., 1994.

18. Venetoklis, P.S., Paniagua, J.C., "Solar System Exploration Utilizing a Particle Bed Reactor Propulsion System", IAF 92-0555, 43d Congress of the International Astronautical Federation, Washington, D.C., September, 1992.

19. "Project Galileo, Bring Jupiter to Earth", http://www.jpl.nasa.gov/galileo.

20. "Cassini, Mission to Saturn", http://www.jpl.nasa.gov/cassini.

21. Isakowitz, Steven, ed. International Reference Guide to Space Launch Systems, 2nd ed., Washington, D.C., American Institute of Aeronautics and Astronautics, 1995.

22. Venetoklis, P.S., Paniagua, J.C., "A Planetary Capture Vehicle Based on a Particle Bed Reactor Propulsion System", AIAA 92-3408, AIAA/SAE/ASME, 28th Joint Propulsion Conf., Nashville, TN, July, 1992.

23. National Space Council, "America at the Threshold," America's Space Exploration Initiative (Stafford Group), Report of the Synthesis Group, USGPO, Washington, DC, 1991.

24. National Aeronautics and Space Administration, "90 Day Study on Human Exploration of the Moons and Mars," Washington, DC, 1990.

25. Venetoklis, P., Palmer, R., Gustafson E., "Fast Missions to Mars With a Particle Bed Reactor Propulsion System", AIAA 91-3404, AIAA/NASA/OAI Conf. on Adv. SEI Technologies, Cleveland, Ohio, September, 1991.

26. Huber, W.G., Sumrall, J.P., "Establishing the Infrastructure: An Integrated Space Transportation System", Progress in Astronautics and Aeronautics, Mars: Past, Present, and Future, Vol. 145, pp. 195-211, American Institute of Aeronautics and Astronautics, Washington D.C., 1992.

8. LIST OF FIGURES

9. LIST OF TABLES

Table #

10. LIST OF APPENDICES

Appendix A Detailed Neutronic Parameters for MITEE Reactors

Appendix B Detailed Mission Parameters for Selected Examples of Solar System Science and Exploration Missions Utilizing MITEE Nuclear Engines

Table 5.2.1

Examples of Missions to the Outer Planets Enabled by the MITEE Engine

MISSION	Delta V (km/sec)	Launch Date/ Trip Time	IMLEO (kg)	Payload (kg)
Jupiter Orbiter	10.77	Jan. 10, 2006 2 Years	3395 2 Stages/No Restart	600 (Orbiter Spacecraft & Atmospheric Flyer)
Saturn Orbiter	12.37	Oct. 5, 2005 3 Years	4170 2 Stages/No Restart	600 (Orbiter Spacecraft & Atmospheric Flyer)
Europa Lander/ Return Sample	13.53	Jan. 10, 2006 2 Years Outbound 3 Years Return	4610 1 Stage/Restart	200
Pluto Lander/ Return Sample	19.65	Feb. 5, 2005 12 Years Outbound 12 Years Return	9050 1 Stage/Restart	200

Table 5.2.2

Examples of Missions to Pluto Enabled by the MITEE Engine

MISSION	Delta V (km/sec)	Launch Date/ Trip Time	IMLEO (kg)	Payload (kg)
Pluto Fly-By	11.82	Feb. 15, 2005 7 Years	1800 1 Stage/No Restart	200
Pluto Orbiter	17.31	Feb. 3, 2005 13 Years	3985 2 Stages/No Restart	200
Pluto Lander	17.59	Feb. 3, 2005 14 Years	4100 2 Stages/No Restart	200

Table 5.4.1.

Mission Ground Rules and Parameters

Orbits:	
Earth Departure:	407 km Circular
Mars:	250x33,840 km (1 Sol)
Earth Capture:	407x34,500 km
Payloads:	
Habitat:	25 metric tons
Lander & Cargo:	75 metric tons
Crew Size:	6
Reserves:	
ΔV Reserve:	2%
Trapped Propellant:	1%
Performance Reserve:	2%
Consumables in Transit:	4 kg/Man/Day

Table 5.4.2

Mission Analysis Results
(2016 Opposition Mission)

ΔV 's (km/sec)	
Cargo TMI	3.6
Cargo MOC*	2.4
Crew TMI	7.2
Crew MOC	6.9
Crew TEI	7.3
Crew EOC	6.9
Duration (days)	
Cargo E-M	294
Crew E-M	80
Crew Stay	30
Crew M-E	160
Total Crew Transit Time	240
Masses (Metric Tons)	
MTV	172
MCV**	335
ETV	147
1MLEO	654

* Includes 1.2 km/sec for rendezvous
** Excludes mass of ETV, which is part of its payload

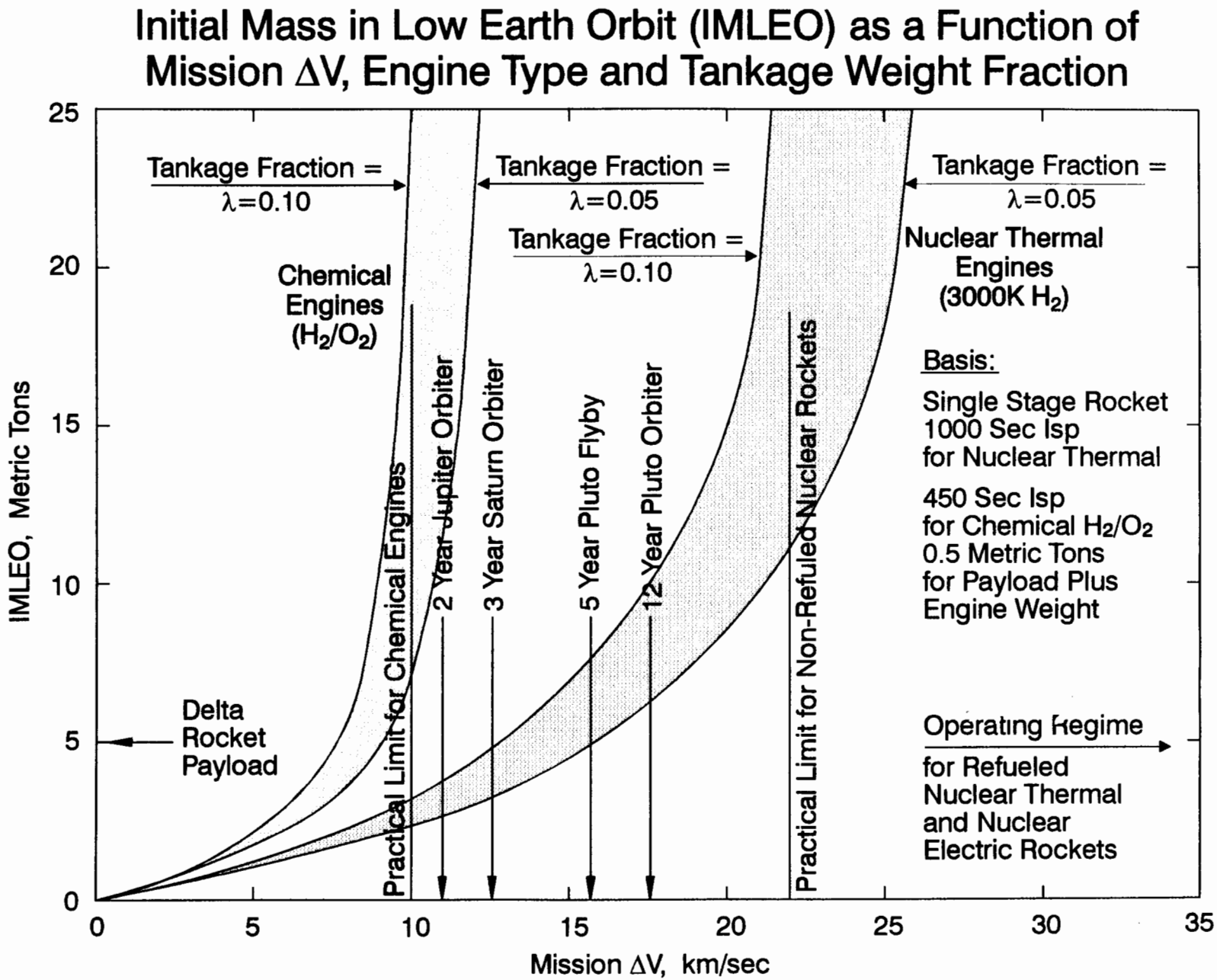
Initial Mass in Low Earth Orbit (IMLEO) as a Function of Mission ΔV, Engine Type and Tankage Weight Fraction
IMLEO, Metric Tons
Mission ΔV, km/sec
0
5
10
15
20
25
30
35
Tankage Fraction = λ=0.10
Tankage Fraction = λ=0.05
Tankage Fraction = λ=0.10
Tankage Fraction = λ=0.05
Chemical Engines (H2/O2)
Nuclear Thermal Engines (3000K H2)
Basis:
Single Stage Rocket
1000 Sec Isp
for Nuclear Thermal
450 Sec Isp
for Chemical H2/O2
0.5 Metric Tons
for Payload Plus
Engine Weight
Delta Rocket Payload
Practical Limit for Chemical Engines
2 Year Jupiter Orbiter
3 Year Saturn Orbiter
5 Year Pluto Flyby
12 Year Pluto Orbiter
Practical Limit for Non-Refuled Nuclear Rockets
Operating Regime
for Refueled Nuclear Thermal and Nuclear Electric Rockets

Figure 2.1

Unique Planetary Missions Enabled by Nuclear Rockets

I. Fast Trip Fly-By and Orbital Capture Missions to Distant Bodies

Potential Missions: Planets (Pluto, etc.), Moons (Titan, etc.), Asteroids, Comets

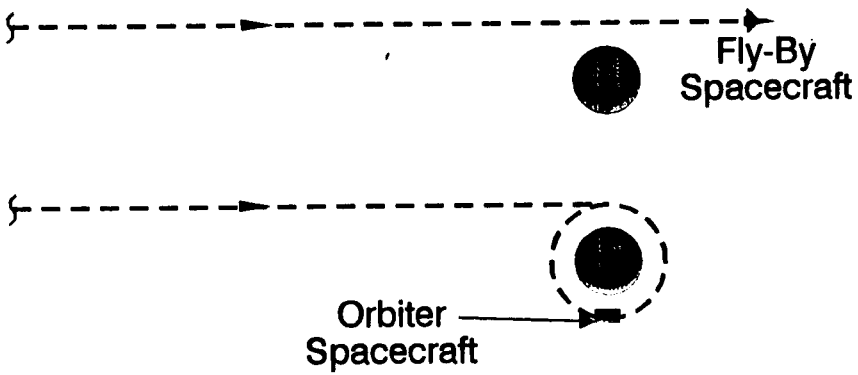

II. Ultra Long Range Planetary Atmospheric Flyers

Potential Missions: Planets (Jupiter, Saturn, etc.), Moons (Titan, etc.)

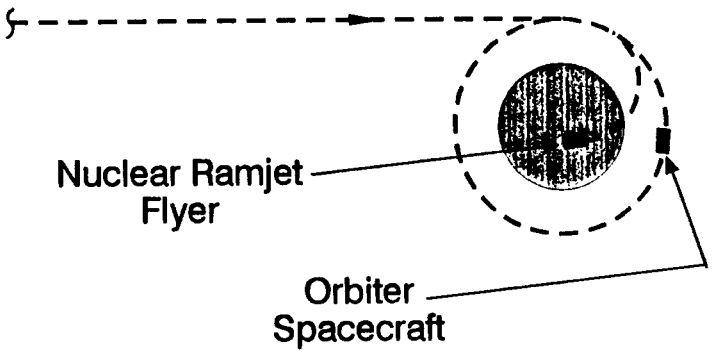

III. Refuel Missions Using Extraterrestrial Propellant Resources to Extend Range or Return Samples

Potential Propellant Sources: Planets (Mars, etc.), Moons (Europa, Titan, etc.), Asteroids, Comets

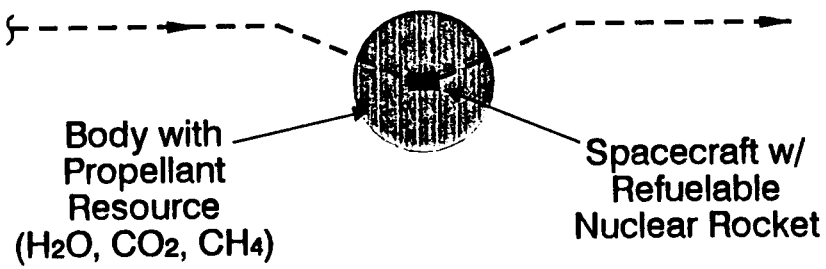

IV. Orbit to Surface Shuttle Missions Using Extraterrestrial Propellant Resources

Potential Shuttle Missions: Planets (Mars), Moons (Earth, etc.)

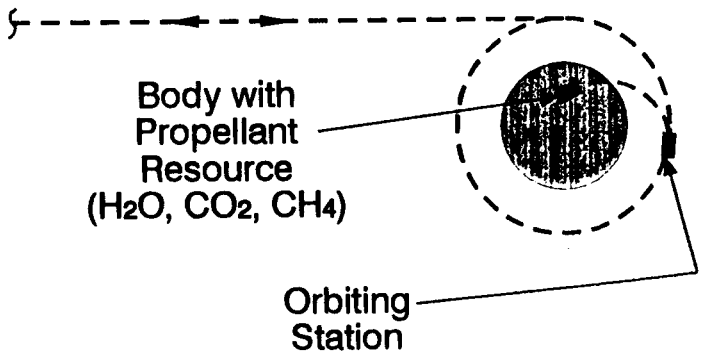

Figure 2.2

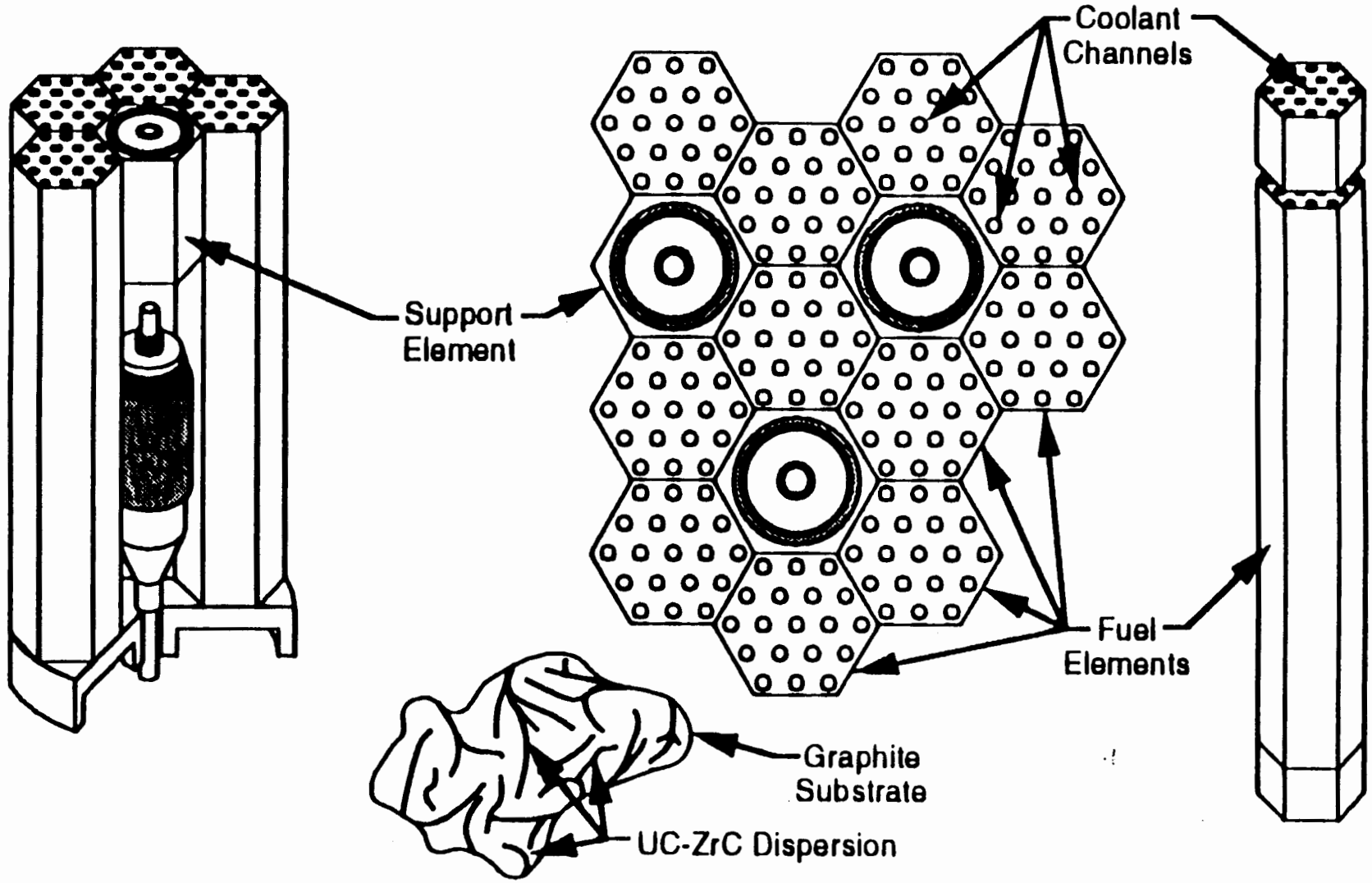

NERVA Reactor Configuration

Figure 3.1A

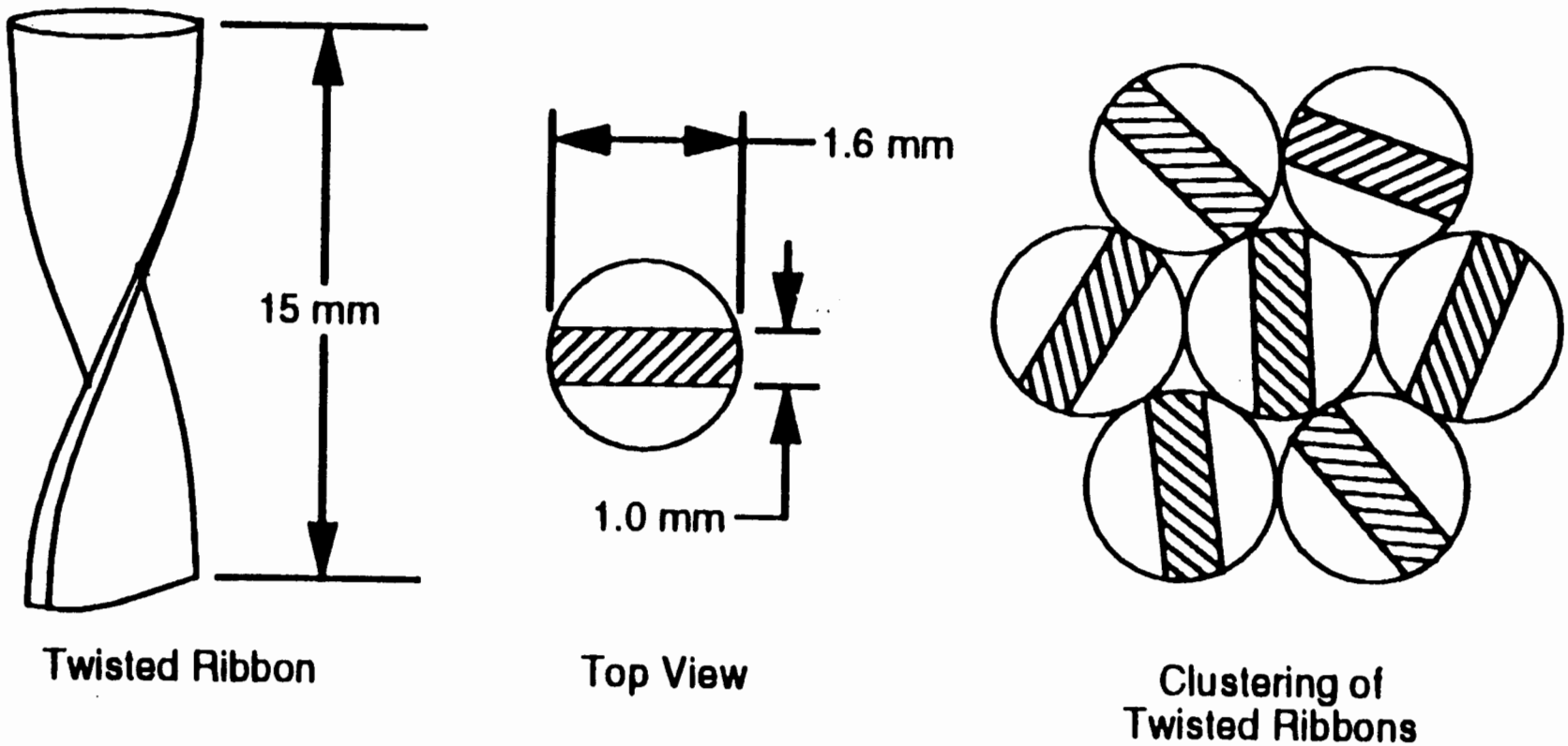

FSU Reactor Concept Configuration

Figure 3.1B

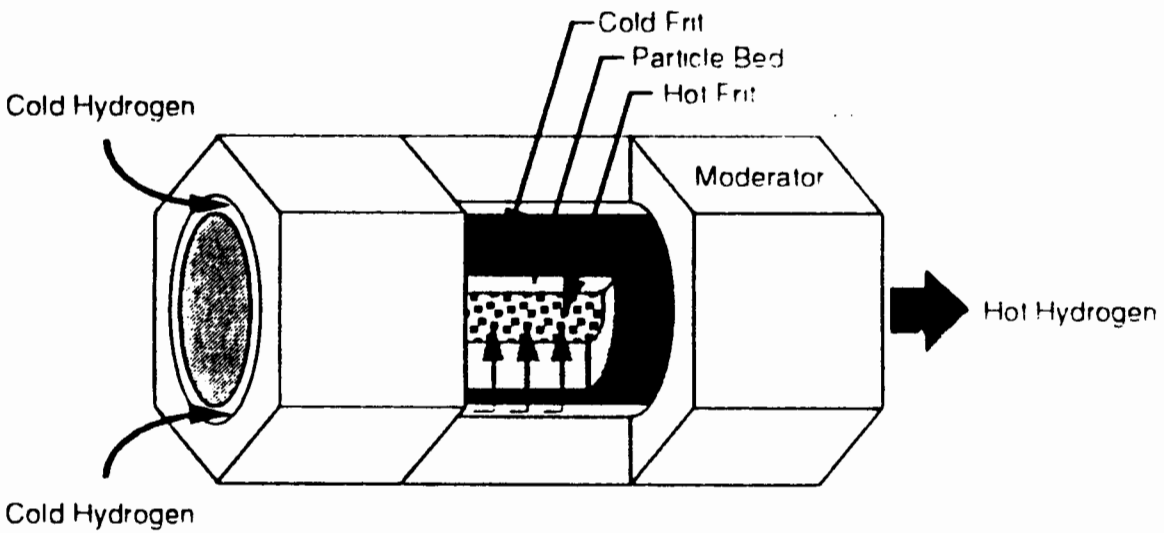

PBR fuel element.

Figure 3.1C

The Particle Bed Reactor

Fuel Particle

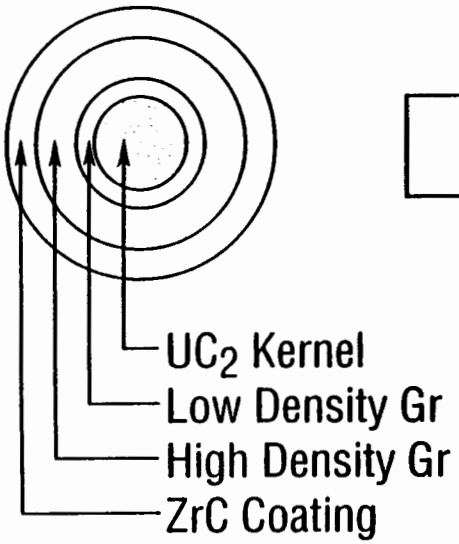

Features:

- 400 μ Diameter
- Melting Point ~ 3000K
- Retains Fission Products

Fuel Element

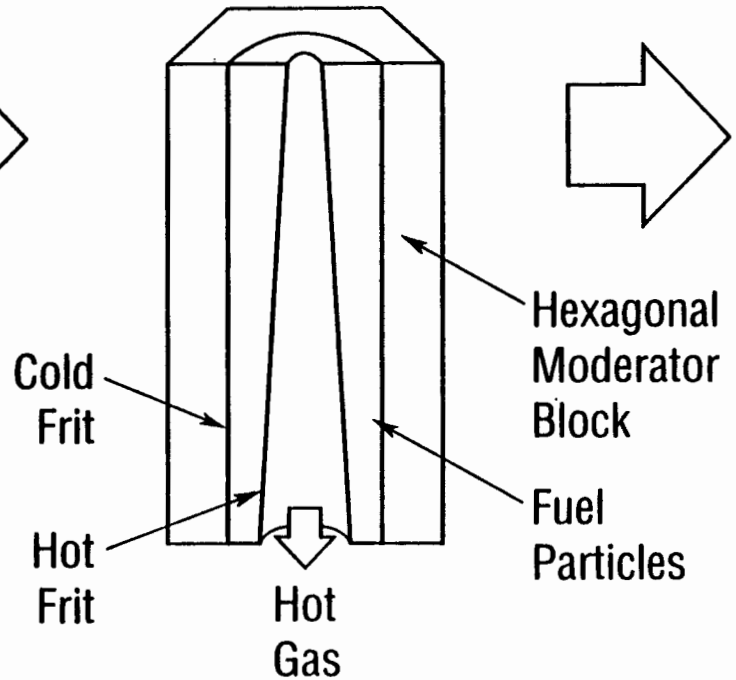

Features:

- Low Gas/Particle Δt
- Gas Heated Directly
- High Po wer Density

Reactor

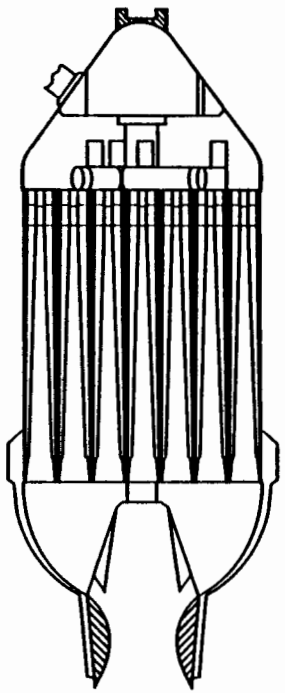

Features:

- Very Compact
- Low Pressure Drop
- Fast Start (<10 Sec)

Figure 3.2

LUDEWIG-1 10/12/93 JNA

PBR Engine Description

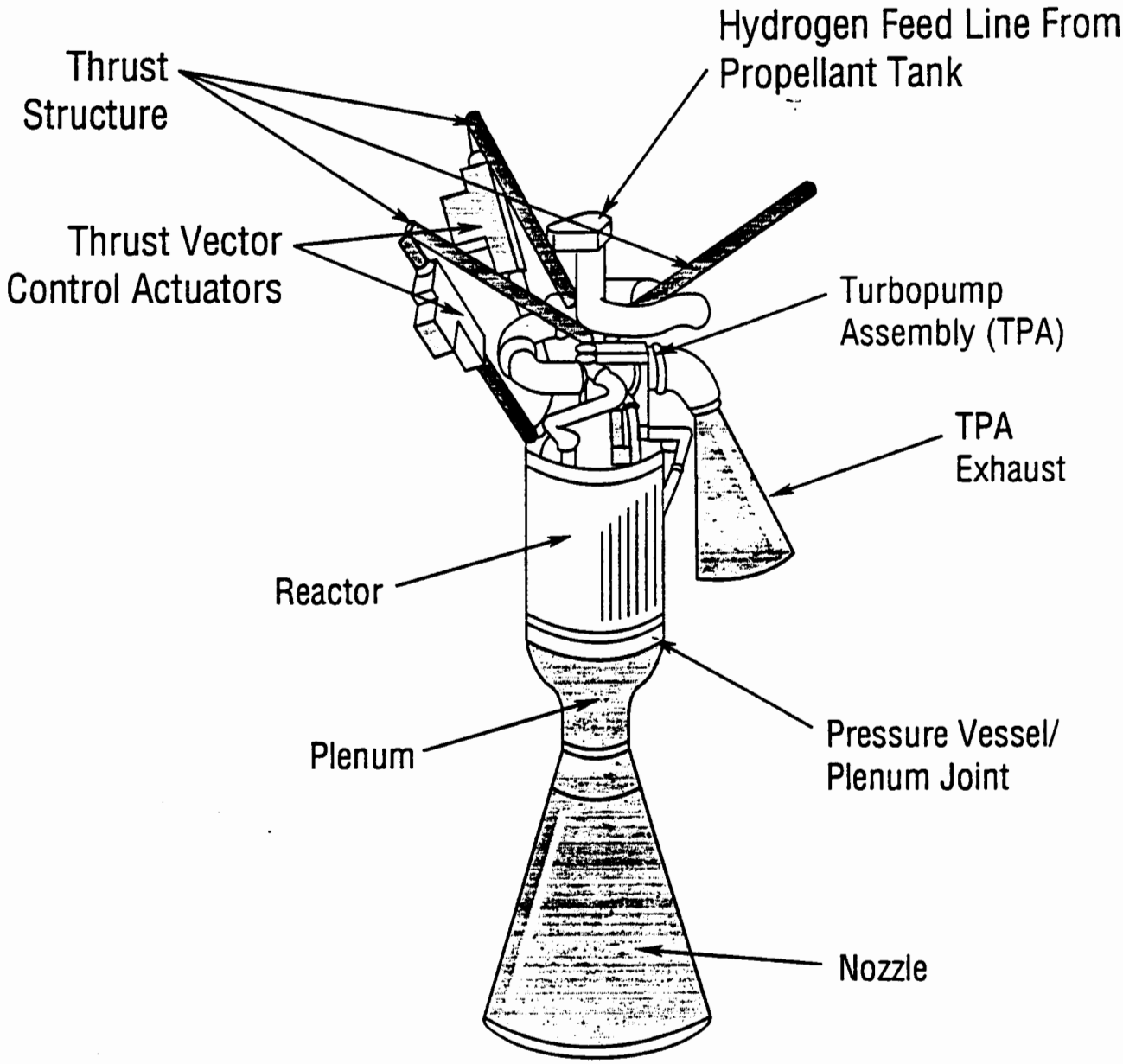

Figure 3.3

LUDEWIG-2 10/12/93 JNA

The MITEE (MIniature ReacTor EnginE) Concept

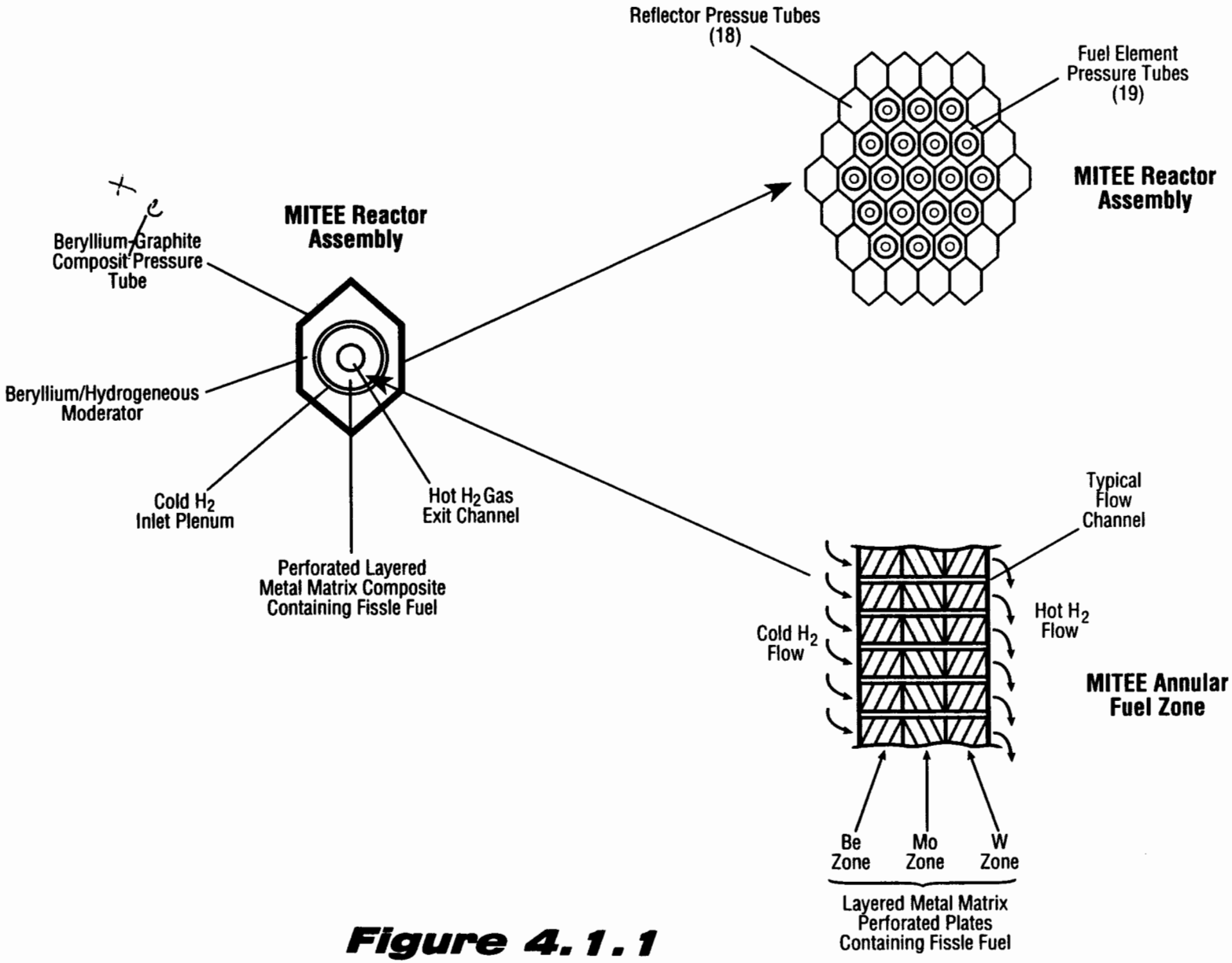

Figure 4.1.1

Powell 1. 9/96 judy

MITEE Pressure Tube and Exit Nozzle

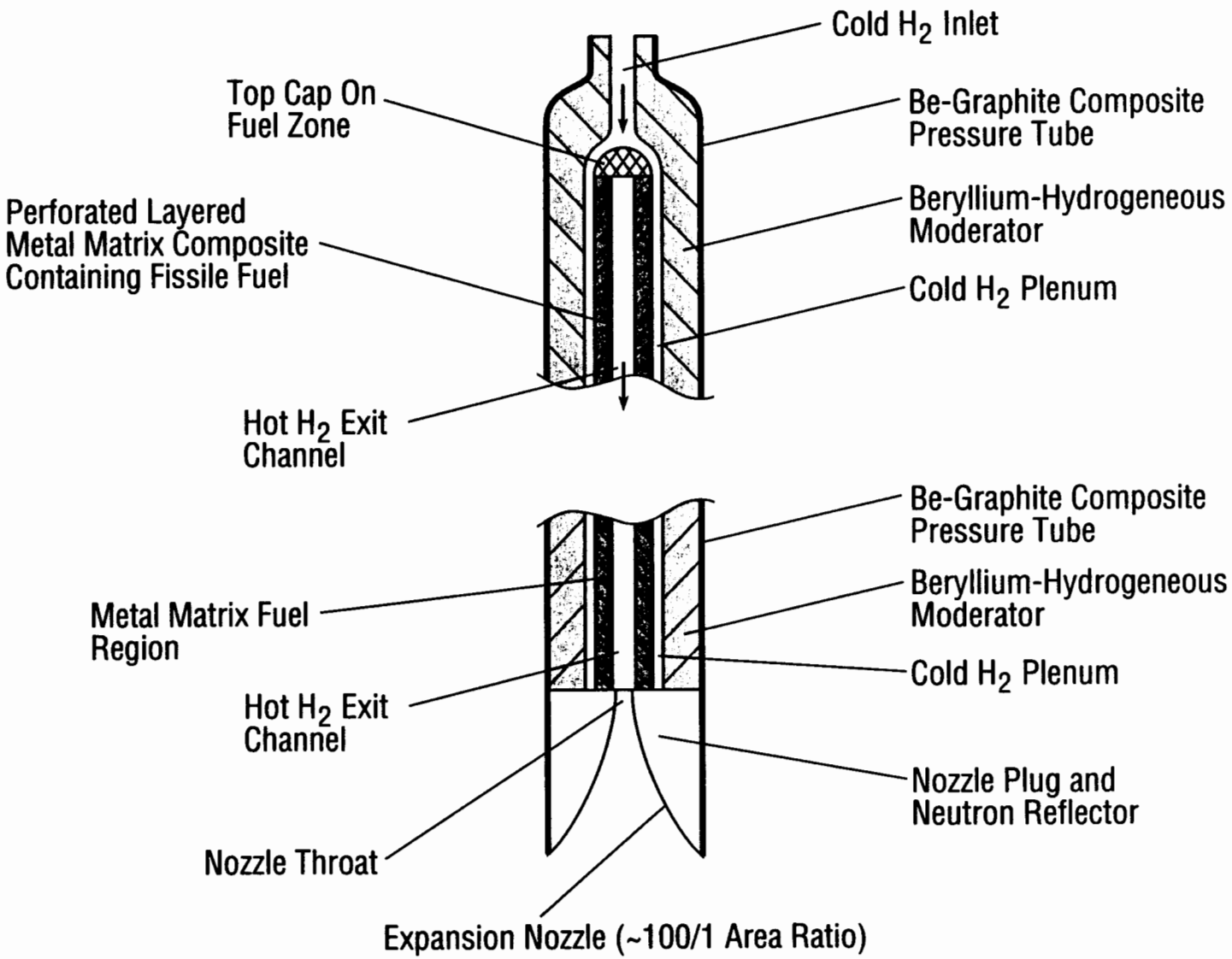

Figure 4.1.2

Construction of Multiple Matrix Sheets

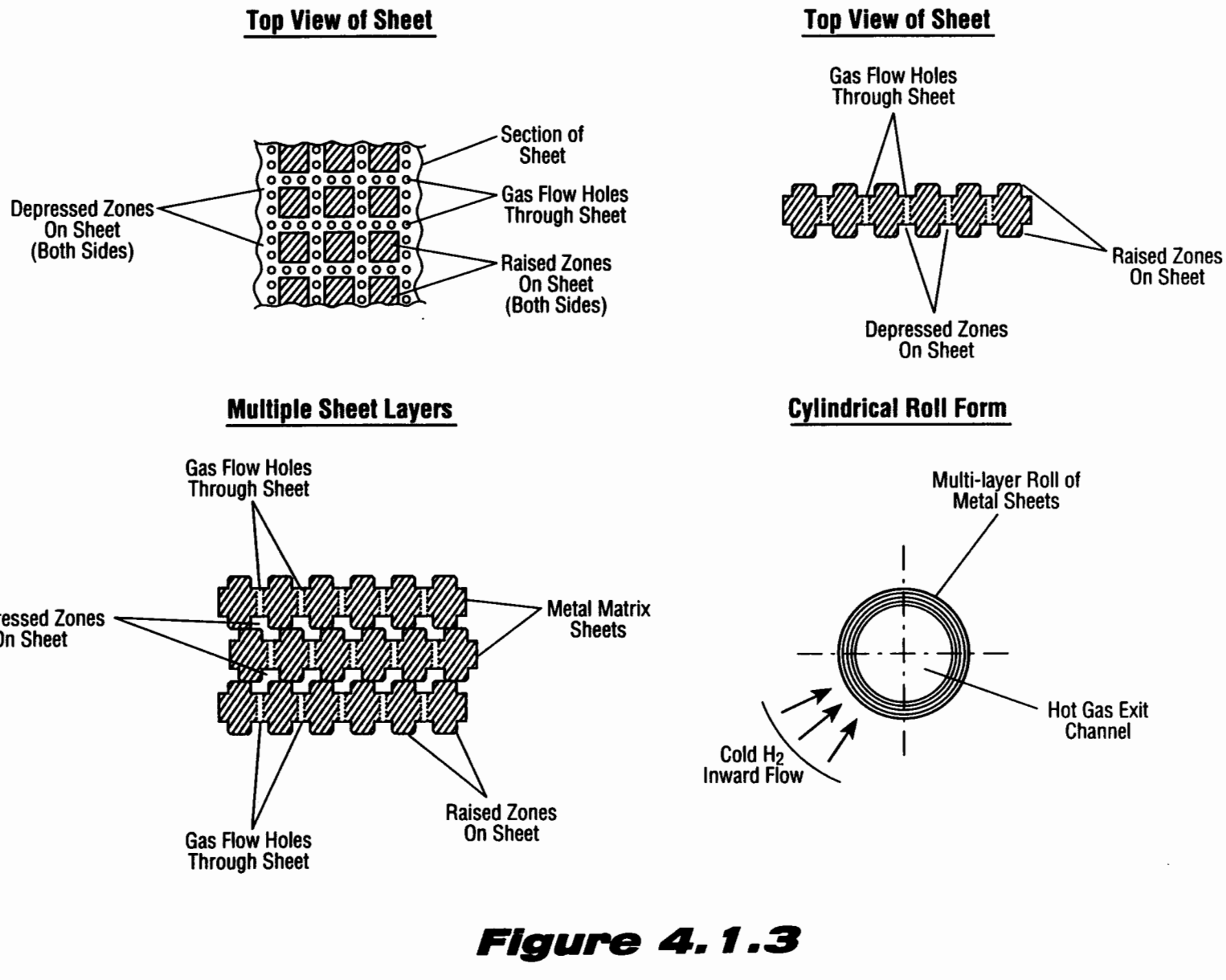

Figure 4.1.3

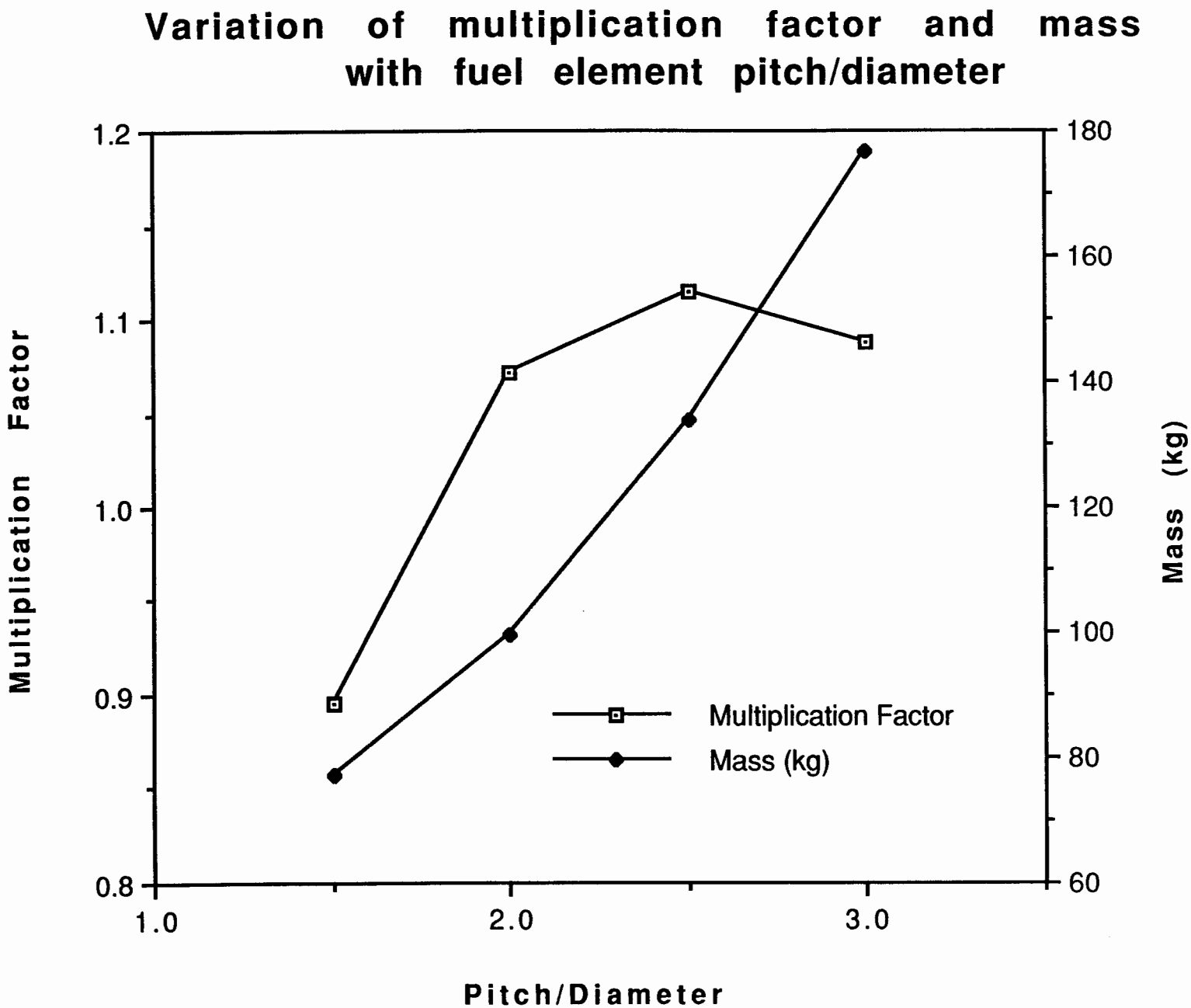
Variation of multiplication factor and mass with fuel element pitch/diameter
Multiplication Factor
Mass (kg)
Pitch/Diameter
1.2
1.1
1.0
0.9
0.8
180
160
140
120
100
80
60
1.0
2.0
3.0
Multiplication Factor
Mass (kg)

Figure 4.2.1

04/28/97 09:34:08
****** MITEE ******

PROBID = 04/28/97 09:34:06
BASIS:
(1.000000, .000000, .000000)
(.000000, 1.000000, .000000)
ORIGIN:
(.00, .00, .00)
EXTENT = (3.00, 3.00)

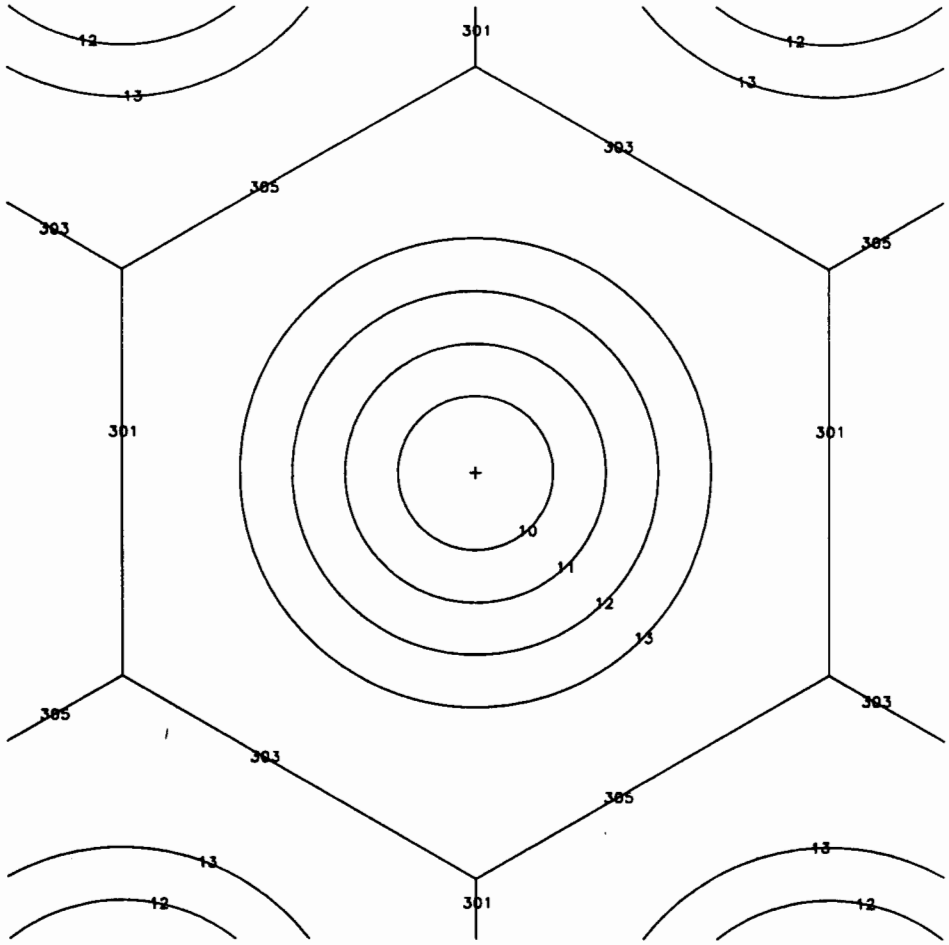

Figure 4.2.2

```
  04/28/97 09:34:12
****** MITEE ******

PROBID =   04/28/97 09:34:06
BASIS:
( 1.000000,  .000000,  .000000)
(  .000000, 1.000000,  .000000)
ORIGIN:
(      .00,      .00,      .00)
EXTENT = (    20.00,    20.00)
```

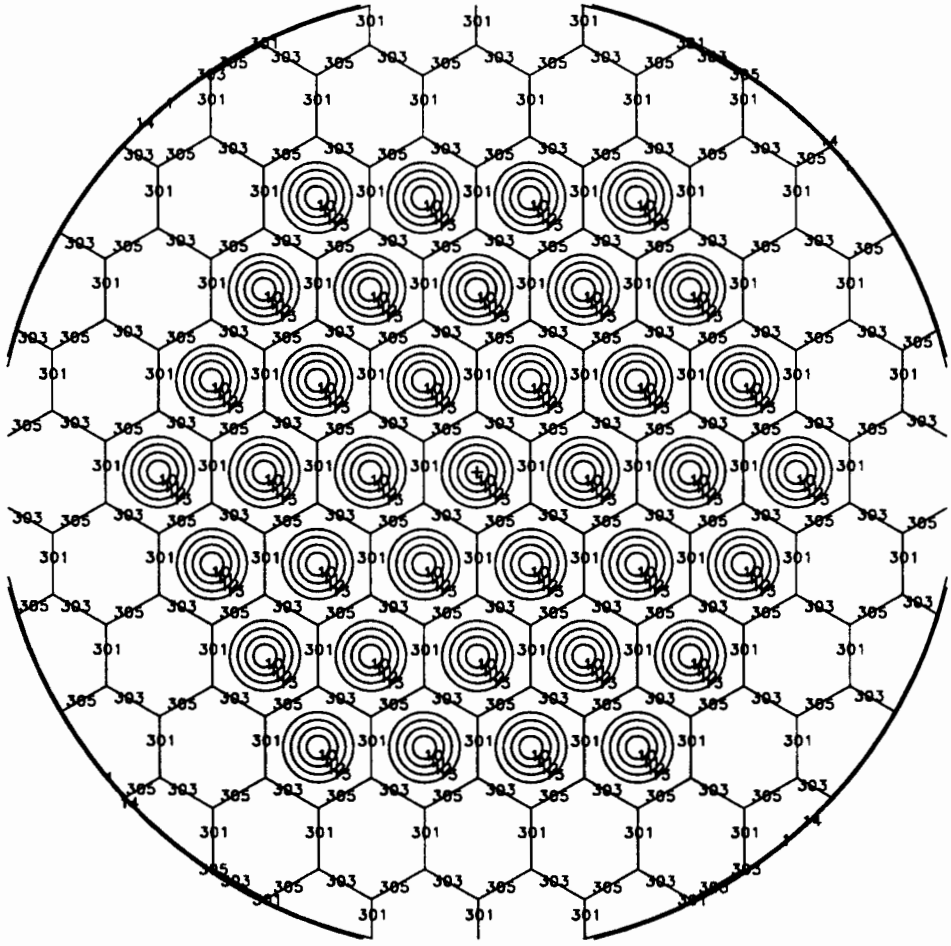

Figure 4.2.3

FUEL SHEET GEOMETRY FOR HEAT TRANSFER ANALYSIS

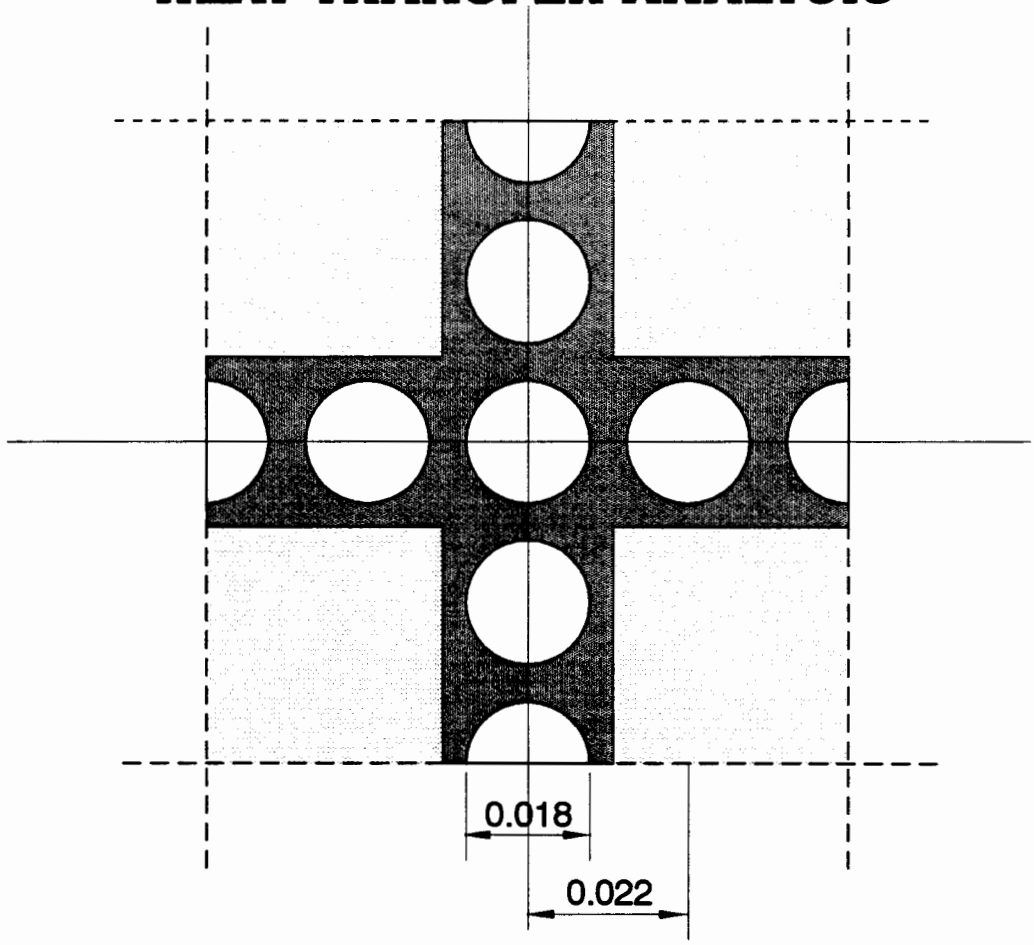

NOTE: ALL DIMENSIONS
ARE IN CM

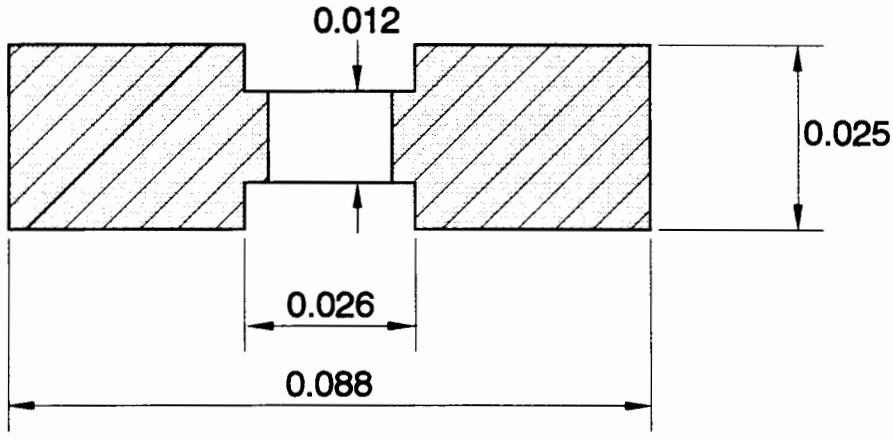

Figure 4.3.1

TEMPERATURE VARIATION THROUGH FUEL REGION OF ANNULAR FUEL ELEMENT

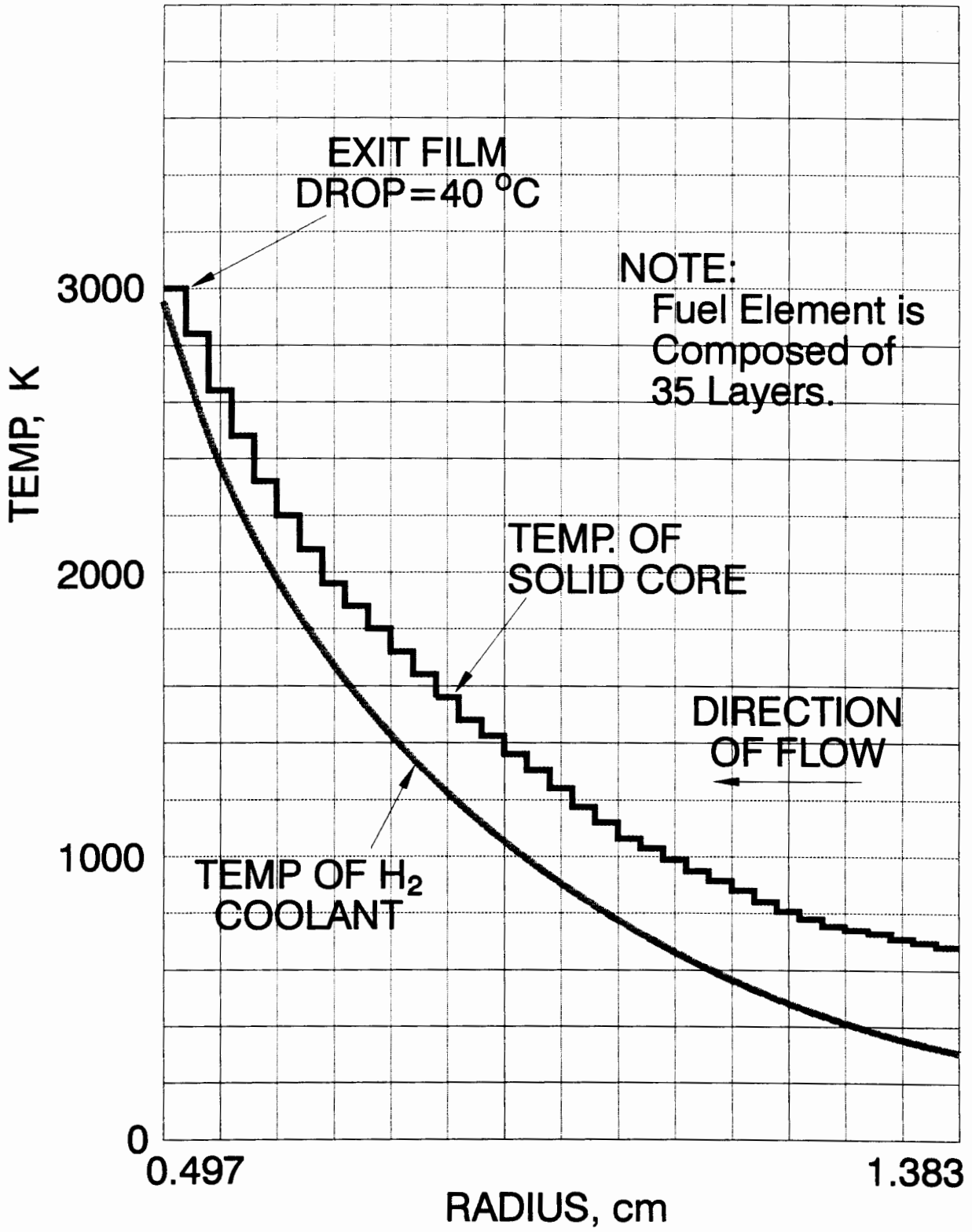

Figure 4.3.2

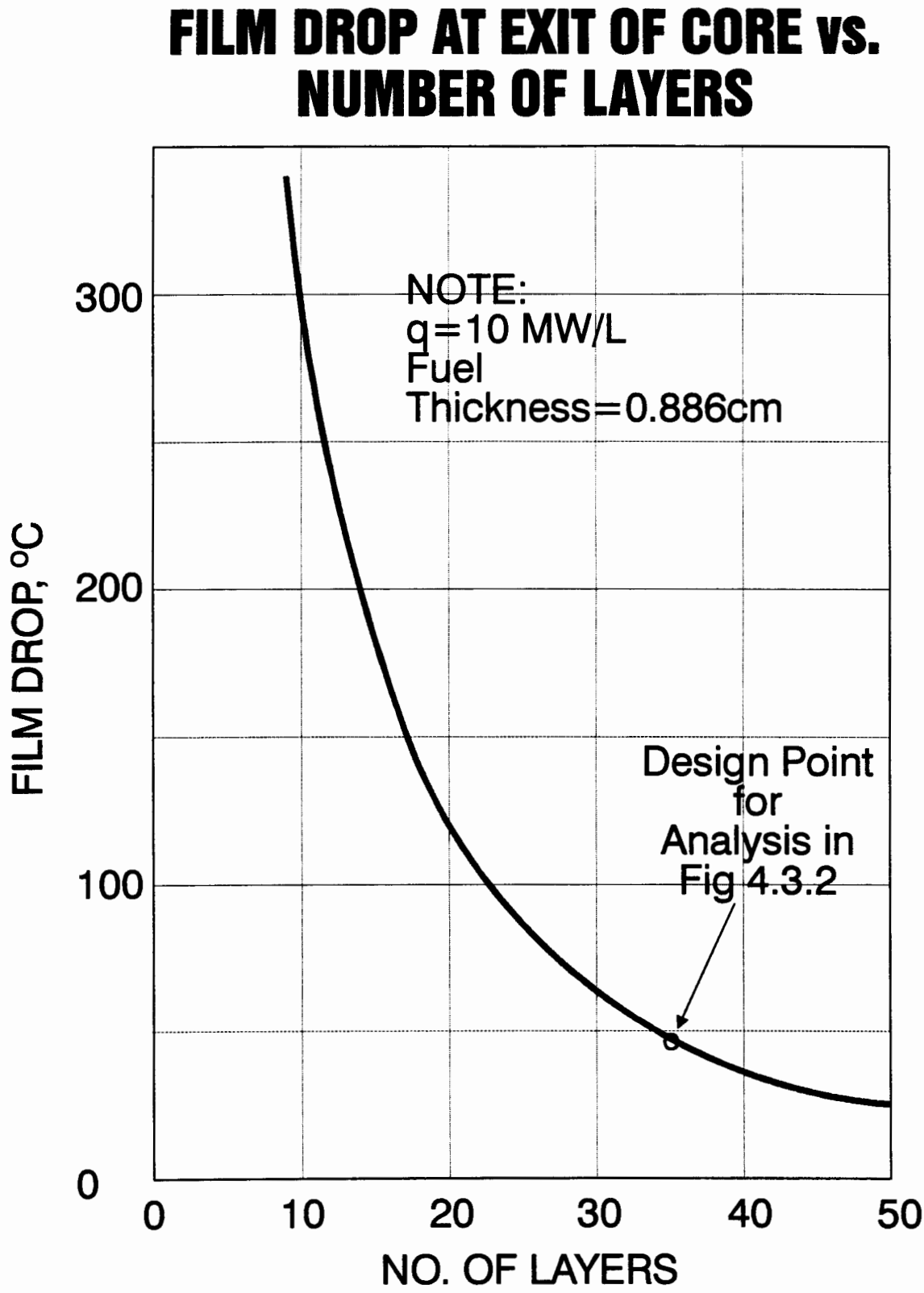
FILM DROP AT EXIT OF CORE vs. NUMBER OF LAYERS
NOTE:
q=10 MW/L
Fuel
Thickness=0.886cm
Design Point for Analysis in Fig 4.3.2
FILM DROP, °C
NO. OF LAYERS
0
100
200
300
0
10
20
30
40
50

Figure 4.3.3

PLUTO MISSIONS USING MITEE NUCLEAR ROCKETS

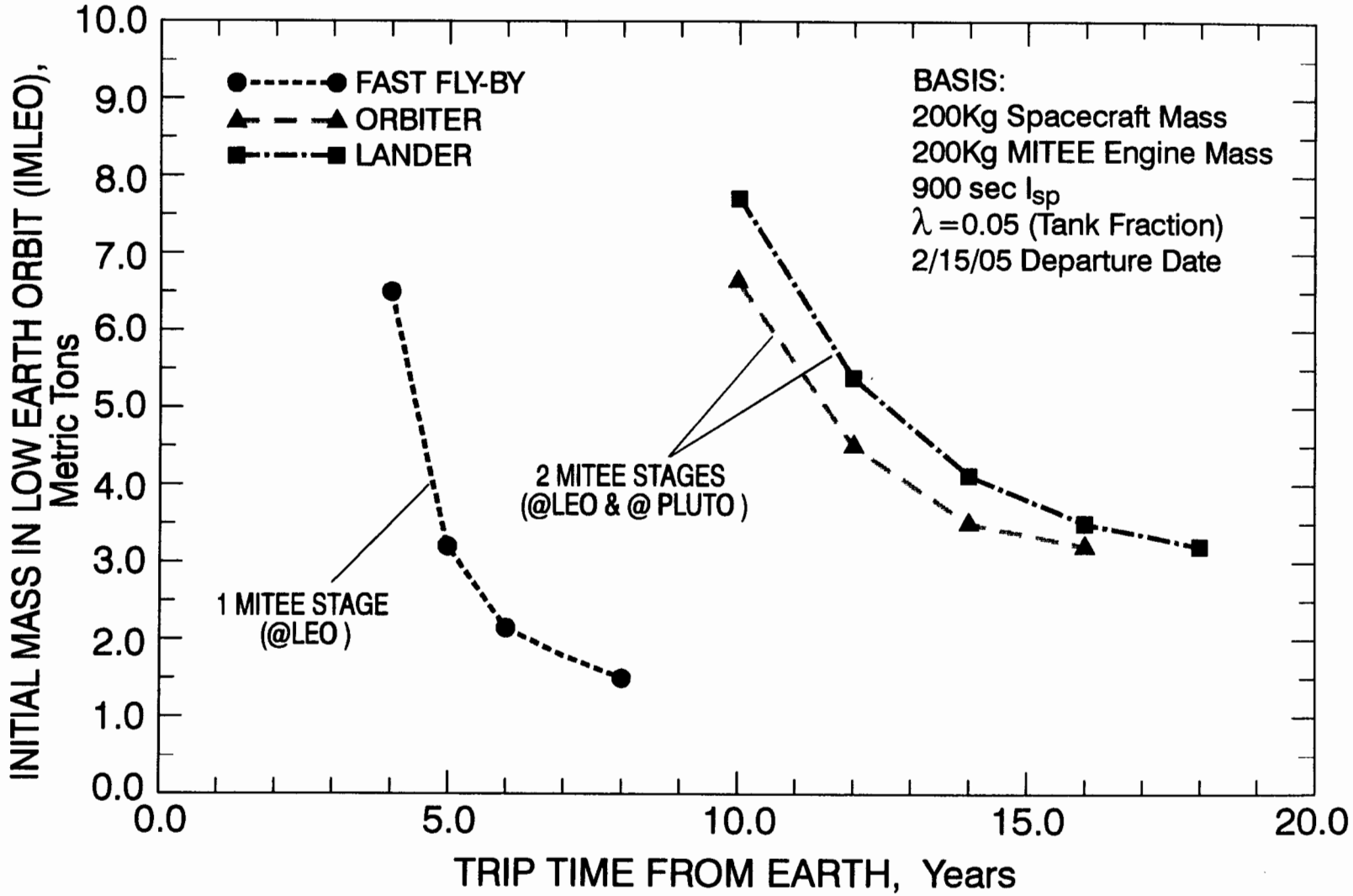

Figure 5.1.1

Launch Vehicle Configurations for MITEE Missions

Fast Fly-By Vehicle Configuration

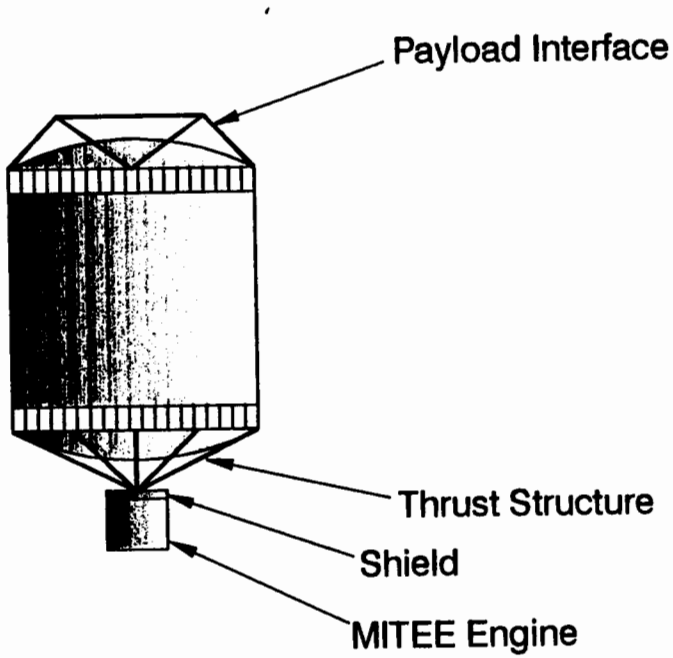

Capture/Lander Vehicle Configuration

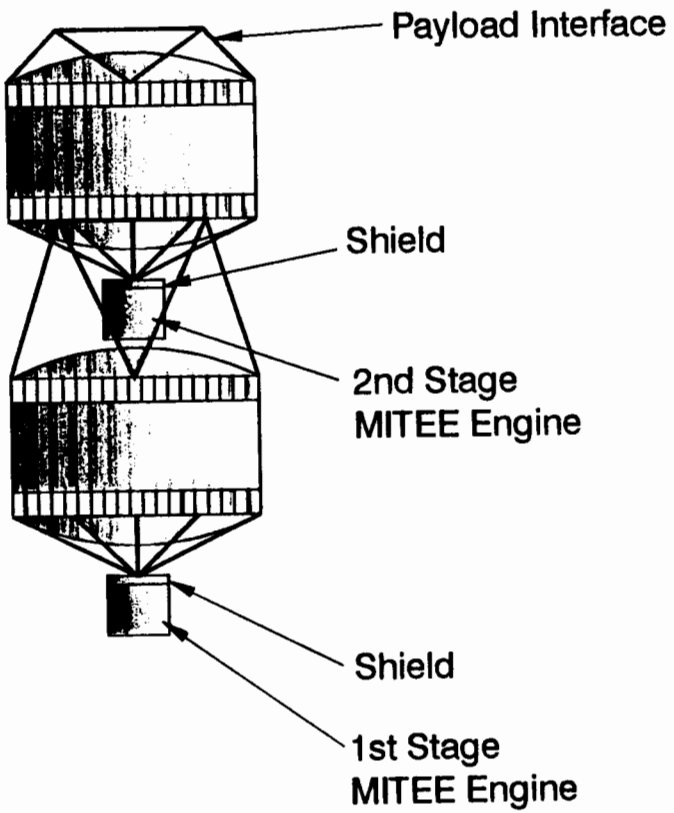

Figure 5.3.1

MARS TRANSFER VEHICLE/EARTH TRANSFER VEHICLE CONFIGURATION

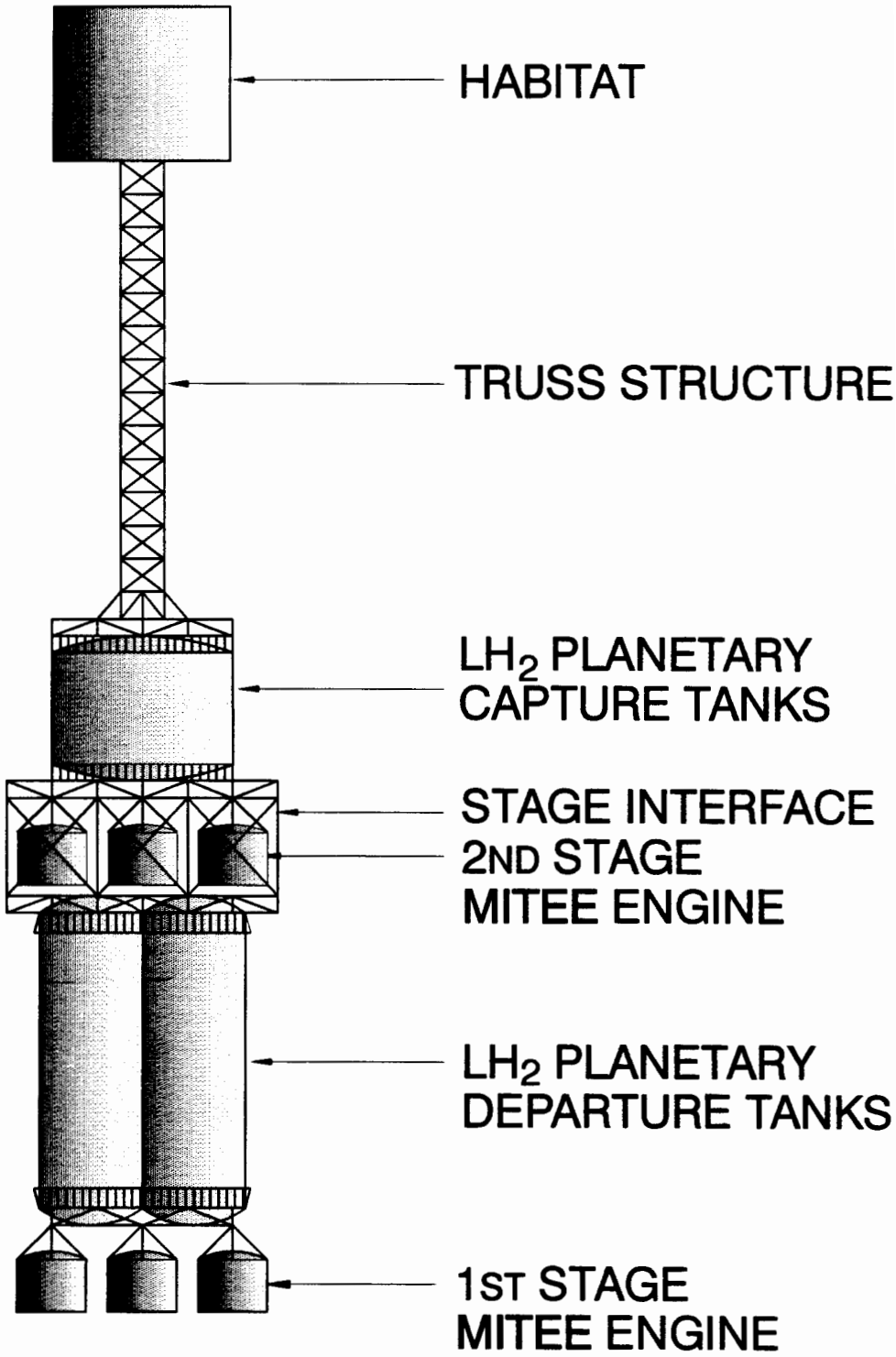

Figure 5.4.1

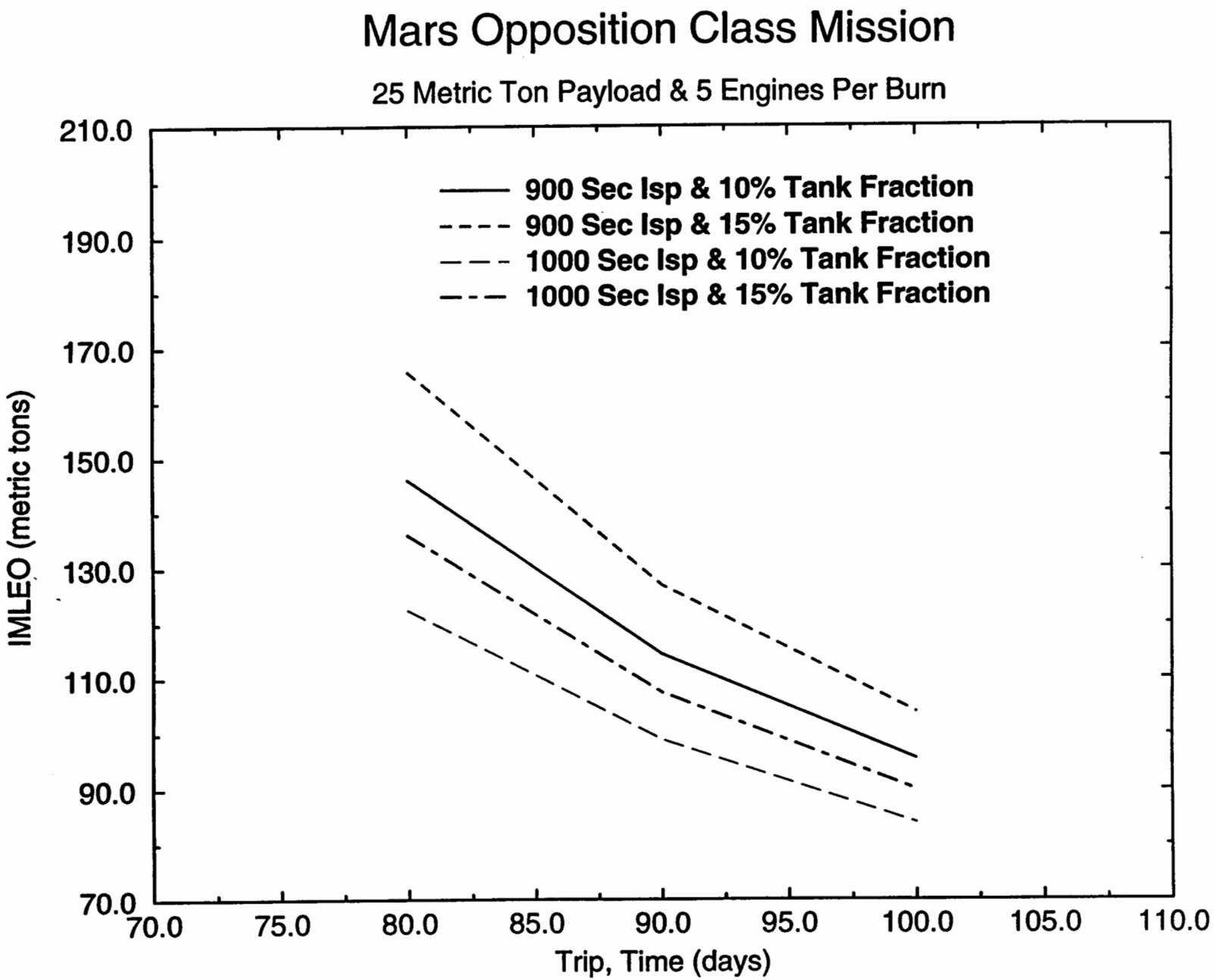
Mars Opposition Class Mission
25 Metric Ton Payload & 5 Engines Per Burn
900 Sec Isp & 10% Tank Fraction
900 Sec Isp & 15% Tank Fraction
1000 Sec Isp & 10% Tank Fraction
1000 Sec Isp & 15% Tank Fraction
IMLEO (metric tons)
210.0
190.0
170.0
150.0
130.0
110.0
90.0
70.0
70.0
75.0
80.0
85.0
90.0
95.0
100.0
105.0
110.0
Trip, Time (days)

Figure 5.4.2

Appendix A

Detailed Neutronic Parameters for MITEE Reactors

"MITEE" Design Formulae (11/07/96)			
Power (kW)	POWER	75	
Propellant Density (kg/m^3)	RHO	0.6103	
Enthalpy Increase (kJ/kg)	DELH	45004	
Sonic Velocity (m/s)	SONICV	3799.5	
Mach Number	MACH	0.25	
Number of Elements	NUMEL	19	
Fuel Element Inner Radius (cm)	RAD1=	0.693982347	
Power density (MW/l)	POWERDEN	10	
	X	2.5	
	Y	5	
	DENOMINATOR	29845.13021	
	A=	1.712835057	
	B=	0.093725993	
Fuel Element Outer Radius (cm)	RAD2=	1.80656105	
Pitch (cm)=(2*X*RAD2)	PITCH=	9.03280525	
Core Height (cm)=Y*pitch	COREH=	45.16402625	
	RADP=	1.064841914	
	RADPP=	1.435701482	
	MASS CALCULATION		
Density UO2 (g/cc)	RHOUO2=	10.2	
Density Tungsten (g/cc)	RHOW=	19.3	
Density Molybdenum (g/cc)	RHOMO=	10.2	
Density Berylium (g/cc)	RHOBE=	1.85	
Tungsten Fraction	TUNGFRAC=	0.23445894	
Molybdenum Fraction	MOLYFRAC=	0.333333333	
Berylium Fraction	BEFRAC=	0.432207727	
	%UO2 in Metal	ff	Mf
	50	0.3	0.3
	40	0.24	0.36
	30	0.18	0.42
	20	0.12	0.48
	10	0.06	0.54
Fuel fraction in cell	ff=	0.3	
Metal fraction in cell	Mf=	0.3	
Average density of fuel (g/cc)	FUELDEN=	5.67739255	
	Mass Fuel=	2241.076007	
Density Liquid H2 (g/cc)	RHOLH2=	0.24	
Density Solid Moderator (g/cc)	RHOSOLID=	0.863	
	RHOMOD=	0.24	
	Mass Moderator=	13880.21494	
Density Reflector (g/cc)	RHOREF=	0.24	
Number of Reflector Elements	NREFL=	37	
	Mass Reflector=	28338.80561	
Thickness of grid plate (cm)	DELT=	3	
	Mass Grid Plate=	7451.136327	

Appendix B

Detailed Mission Parameters for Selected Examples of Solar System Science and Exploration Missions Utilizing MITEE Nuclear Engines

CASE TITLE: Pluto Flyby

FLIGHT TYM: 2555.0 DAYS 6.995 YEARS

MODE: TOTAL DV OPTIMIZATION WITH MASS DATA
RUBBER RETRO STAGE(S)
TERMINAL FLYBY(UNCONSTRAINED)

CENTRAL BODY IS SUN EARTH ECLIPTIC & EQUINOX OF 1950.0

LAUNCH: C3= 264.196 C3PRIME= 264.196
VHL= 16.254 DLA= -4.466 LONG= 146.253

IMPULSES:	NO.	TYM(JD)	BODY	DVX(KPS)	DVY(KPS)	DVZ(KPS)	DV(KPS)
	1	2453417.109	EARTH	ORBIT DEPARTURE			11.872
	2	2455972.109	PLUTO	ORBIT CAPTURE			.000
						TOTAL DV(KPS)=	11.872

IMP POINTS:	NO.	DATE	DAYS	X(AU)	Y(AU)	Z(AU)	R(AU)
	1	2005 FEB 15	.0	-.8214	.5488	-.0001	.9878
	2	2012 FEB 14	2555.0	3.8344	-31.7519	2.1889	32.0574

AUX DATA:	NO.	VHP(KPS)	DEC(DEG)	RA(DEG)	PHAZ(DEG)	SET(DEG)	RC(AU)
	1*	16.254	-4.466	235.135	87.250	.000	.0000
	2*	18.958	43.138	30.971	13.045	46.397	32.7305

* = BODY EQUATORIAL VHP COORDINATES

MASS DATA:	STAGE	DV(KPS)	MR(KG)	MP(KG)	MPMAX(KG)		
	1	11.872	1590.	1323.	99999.	MOMAX(KG)=	1790.
						MO(KG)=	1790.
						PAYLOAD(KG)=	200.

RUN DATA:	NO.	TYM GRAD	POSXGRAD	POSYGRAD	POSZGRAD
	1	-.899E-08	.000E+00	.000E+00	.000E+00
	2	.000E+00	.000E+00	.000E+00	.000E+00

NS= 1 0 1 0 1 7
NRI= 0

*** **********

CASE TITLE: Pluto Capture

FLIGHT TYM: 4745.0 DAYS 12.991 YEARS

MODE: TOTAL DV OPTIMIZATION WITH MASS DATA
RUBBER RETRO STAGE(S)
TERMINAL PLANET CAPTURE

CENTRAL BODY IS SUN EARTH ECLIPTIC & EQUINOX OF 1950.0

LAUNCH: C3= 158.438 C3PRIME= 158.438
VHL= 12.587 DLA= -13.561 LONG= 134.469

IMPULSES: NO.	TYM(JD)	BODY	DVX(KPS)	DVY(KPS)	DVZ(KPS)	DV(KPS)
1	2453405.465	EARTH	ORBIT DEPARTURE			8.947
2	2458150.465	PLUTO	ORBIT CAPTURE			8.363
					TOTAL DV(KPS)=	17.310

IMP POINTS: NO.	DATE	DAYS	X(AU)	Y(AU)	Z(AU)	R(AU)
1	2005 FEB 3	.0	-.6906	.7035	-.0001	.9858
2	2018 JAN 31	4745.0	10.6260	-31.6245	.1998	33.3626

AUX DATA: NO.	VHP(KPS)	DEC(DEG)	RA(DEG)	PHAZ(DEG)	SET(DEG)	RC(AU)
1*	12.587	-13.561	222.424	89.126	.000	.0000
2*	9.039	42.023	27.357	27.891	21.885	34.2749

* = BODY EQUATORIAL VHP COORDINATES

MASS DATA: STAGE	DV(KPS)	MR(KG)	MP(KG)	MPMAX(KG)	
1	8.947	2865.	2538.	99999.	MOMAX(KG)= 3985.
2	8.363	920.	686.	99999.	MO(KG)= 3985.
					PAYLOAD(KG)= 200.

RUN DATA: NO.	TYM GRAD	POSXGRAD	POSYGRAD	POSZGRAD
1	-.324E-07	.000E+00	.000E+00	.000E+00
2	.000E+00	.000E+00	.000E+00	.000E+00

NS= 1 0 1 0 1 6
NRI= 0

CASE TITLE: Jupiter Capture

FLIGHT TYM: 730.0 DAYS 1.999 YEARS

MODE: TOTAL DV OPTIMIZATION WITH MASS DATA
RUBBER RETRO STAGE(S)
TERMINAL PLANET CAPTURE

CENTRAL BODY IS SUN EARTH ECLIPTIC & EQUINOX OF 1950.0

LAUNCH: C3= 80.717 C3PRIME= 80.717
VHL= 8.984 DLA= -4.523 LONG= 109.206

IMPULSES: NO.	TYM(JD)	BODY	DVX(KPS)	DVY(KPS)	DVZ(KPS)	DV(KPS)
1	2453745.882	EARTH		ORBIT DEPARTURE		6.418
2	2454475.882	JUPIT		ORBIT CAPTURE		4.357
					TOTAL DV(KPS)=	10.774

IMP POINTS: NO.	DATE	DAYS	X(AU)	Y(AU)	Z(AU)	R(AU)
1	2006 JAN 10	.0	-.3235	.9287	-.0001	.9834
2	2008 JAN 10	730.0	.1442	-5.2409	.0176	5.2429

AUX DATA: NO.	VHP(KPS)	DEC(DEG)	RA(DEG)	PHAZ(DEG)	SET(DEG)	RC(AU)
1*	8.984	-4.523	197.447	88.121	.000	.0000
2*	7.636	3.801	88.095	46.960	14.429	6.1895

* = BODY EQUATORIAL VHP COORDINATES

MASS DATA: STAGE	DV(KPS)	MR(KG)	MP(KG)	MPMAX(KG)		
1	6.418	2041.	1754.	99999.	MOMAX(KG)=	3395.
2	4.357	754.	527.	99999.	MO(KG)=	3395.
					PAYLOAD(KG)=	600.

RUN DATA: NO.	TYM GRAD	POSXGRAD	POSYGRAD	POSZGRAD
1	-.209E-07	.000E+00	.000E+00	.000E+00
2	.000E+00	.000E+00	.000E+00	.000E+00

NS= 1 0 1 0 1 7
NRI= 0

```
********************************************************************************
CASE TITLE: Saturn Capture

FLIGHT TYM:          1095.0 DAYS          2.998 YEARS

      MODE: TOTAL DV OPTIMIZATION WITH MASS DATA
            RUBBER RETRO STAGE(S)
            TERMINAL PLANET CAPTURE

            CENTRAL BODY IS SUN          EARTH ECLIPTIC & EQUINOX OF 1950.0

    LAUNCH:     C3=  133.913   C3PRIME=  133.913
              VHL=   11.572       DLA=   37.029      LONG=   11.561

  IMPULSES:  NO.     TYM(JD)       BODY     DVX(KPS)   DVY(KPS)   DVZ(KPS)   DV(KPS)

               1  2453648.986     EARTH           ORBIT DEPARTURE              8.178
               2  2454743.986     SATUR           ORBIT CAPTURE                4.190
                                                                  ------------------------
                                                                   TOTAL DV(KPS)=  12.367
                                                                  ------------------------

IMP POINTS:  NO.       DATE        DAYS       X(AU)      Y(AU)      Z(AU)      R(AU)

               1  2005 OCT  5         .0      .9796      .2004      .0000      .9999
               2  2008 OCT  4     1095.0    -8.8836     2.8395      .3072     9.3314

  AUX DATA:  NO.      VHP(KPS)   DEC(DEG)   RA(DEG)   PHAZ(DEG)   SET(DEG)    RC(AU)

               1*       11.572     37.029     98.716     85.248       .000      .0000
               2*       10.224     15.814    139.569     32.357     25.903    10.2209
                * = BODY EQUATORIAL VHP COORDINATES

 MASS DATA: STAGE      DV(KPS)     MR(KG)     MP(KG)   MPMAX(KG)

               1         8.178       2844.      2518.     99999.    MOMAX(KG)=  4170.
               2         4.190        726.       501.     99999.       MO(KG)=  4170.
                                                                  --------------------
                                                                   PAYLOAD(KG)=   600.
                                                                  --------------------

  RUN DATA:  NO.     TYM GRAD   POSXGRAD   POSYGRAD   POSZGRAD

               1    -.512E-07   .000E+00   .000E+00   .000E+00
               2     .000E+00   .000E+00   .000E+00   .000E+00

              NS=        1    0    1    0    1    6
             NRI=        0
```

```
**********************************************************************************
CASE TITLE: Europa Capture

FLIGHT TYM:            730.0 DAYS          1.999 YEARS

      MODE: TOTAL DV OPTIMIZATION WITH MASS DATA
            RUBBER RETRO STAGE(S)
            TERMINAL PLANET CAPTURE

            CENTRAL BODY IS SUN          EARTH ECLIPTIC & EQUINOX OF 1950.0

    LAUNCH:     C3=   80.734   C3PRIME=   80.734
              VHL=    8.985      DLA=   -4.492      LONG=  109.446

  IMPULSES:  NO.     TYM(JD)       BODY     DVX(KPS)  DVY(KPS)  DVZ(KPS)   DV(KPS)

               1  2453746.118     EARTH          ORBIT DEPARTURE             6.418
               2  2454476.118     JUPIT          ORBIT CAPTURE               9.244
                                                                ------------------------
                                                                 TOTAL DV(KPS)=  15.662
                                                                ------------------------

IMP POINTS:  NO.       DATE        DAYS       X(AU)      Y(AU)      Z(AU)      R(AU)

               1  2006 JAN 10         .0     -.3274      .9273     -.0001      .9834
               2  2008 JAN 10      730.0      .1460    -5.2407      .0175     5.2428

  AUX DATA:  NO.      VHP(KPS)  DEC(DEG)  RA(DEG)  PHAZ(DEG)  SET(DEG)   RC(AU)

               1*        8.985    -4.492  197.269     87.705      .000      .0000
               2*        7.633     3.810   88.089     46.986    14.616     6.1885
                * = BODY EQUATORIAL VHP COORDINATES

 MASS DATA: STAGE      DV(KPS)     MR(KG)     MP(KG)  MPMAX(KG)

               1       15.662      4410.      3828.     99999.    MOMAX(KG)=  4610.
                                                                      MO(KG)=  4610.
                                                                ---------------------
                                                                 PAYLOAD(KG)=   200.
                                                                ---------------------

  RUN DATA:  NO.     TYM GRAD  POSXGRAD  POSYGRAD  POSZGRAD

               1    -.196E-07  .000E+00  .000E+00  .000E+00
               2     .000E+00  .000E+00  .000E+00  .000E+00

              NS=       1    0    1    0    1    7
             NRI=       0
```

```
**********************************************************************
CASE TITLE: Direct Earth to Mars

FLIGHT TYM:              80.0 DAYS            .219 YEARS

     MODE: TOTAL DV OPTIMIZATION WITH MASS DATA
           RUBBER RETRO STAGE(S)
           TERMINAL PLANET CAPTURE

           CENTRAL BODY IS SUN          EARTH ECLIPTIC & EQUINOX OF 1950.0

   LAUNCH:     C3=  103.773   C3PRIME=  103.773
              VHL=   10.187       DLA=  -19.781      LONG=  215.713

 IMPULSES:  NO.     TYM(JD)       BODY     DVX(KPS)  DVY(KPS)  DVZ(KPS)  DV(KPS)

             1  2457504.949     EARTH          ORBIT DEPARTURE             7.210
             2  2457584.949     MARS           ORBIT CAPTURE               6.907
                                                                ------------------------
                                                                TOTAL DV(KPS)=  14.117
                                                                ------------------------

IMP POINTS:  NO.       DATE        DAYS       X(AU)      Y(AU)      Z(AU)      R(AU)

             1  2016 APR 26          .0     -.8171     -.5875      .0001     1.0064
             2  2016 JUL 15        80.0      .0116    -1.4526     -.0310     1.4529

 AUX DATA:  NO.      VHP(KPS)  DEC(DEG)  RA(DEG)  PHAZ(DEG)  SET(DEG)   RC(AU)

             1*       10.187   -19.781   218.190      7.441      .000      .0000
             2*       10.464    -5.874   344.848     22.304   121.232      .6373
              * = BODY EQUATORIAL VHP COORDINATES

MASS DATA:  STAGE     DV(KPS)     MR(KG)     MP(KG)  MPMAX(KG)

             1         7.210     106785.     95986.     99999.   MOMAX(KG)=172000.
             2         6.907      40125.     35387.     99999.      MO(KG)=172000.
                                                                ------------------------
                                                                PAYLOAD(KG)= 25090.
                                                                ------------------------
 RUN DATA:  NO.     TYM GRAD  POSXGRAD  POSYGRAD  POSZGRAD

             1    -.440E-06  .000E+00  .000E+00  .000E+00
             2     .000E+00  .000E+00  .000E+00  .000E+00

            NS=       1    0    1    0    1    6
           NRI=       0
```

CASE TITLE: Earth to Mars - Cargo

FLIGHT TYM: 294.0 DAYS .805 YEARS

MODE: NO OPTIMIZATION IN EFFECT
TERMINAL PLANET CAPTURE

CENTRAL BODY IS SUN EARTH ECLIPTIC & EQUINOX OF 1950.0

LAUNCH: C3= 9.379 C3PRIME= 9.379
VHL= 3.063 DLA= 27.250 LONG= 75.670

IMPULSES: NO.	TYM(JD)	BODY	DVX(KPS)	DVY(KPS)	DVZ(KPS)	DV(KPS)
1	2456635.000	EARTH		ORBIT DEPARTURE		3.599
2	2456929.000	MARS		ORBIT CAPTURE		2.390
					TOTAL DV(KPS)=	5.990

IMP POINTS: NO.	DATE	DAYS	X(AU)	Y(AU)	Z(AU)	R(AU)
1	2013 DEC 8	.0	.2438	.9544	-.0001	.9850
2	2014 SEP 28	294.0	.4550	-1.3440	-.0395	1.4195

AUX DATA: NO.	VHP(KPS)	DEC(DEG)	RA(DEG)	PHAZ(DEG)	SET(DEG)	RC(AU)
1*	3.063	27.250	200.880	107.707	.000	.0000
2*	3.190	-34.158	295.527	92.974	64.665	1.5218

* = BODY EQUATORIAL VHP COORDINATES

MASS DATA: STAGE	DV(KPS)	MR(KG)	MP(KG)	MPMAX(KG)	
1	3.599	178989.	161353.	99999.	MOMAX(KG)=482000.
2	2.390	80552.	71865.	99999.	MO(KG)=482000.
					PAYLOAD(KG)=222459.

RUN D

*** **********

CASE TITLE: Direct Mars to Earth

FLIGHT TYM: 160.0 DAYS .438 YEARS

MODE: NO OPTIMIZATION IN EFFECT
TERMINAL PLANET CAPTURE

CENTRAL BODY IS SUN EARTH ECLIPTIC & EQUINOX OF 1950.0

IMPULSES:	NO.	TYM(JD)	BODY	DVX(KPS)	DVY(KPS)	DVZ(KPS)	DV(KPS)
	1	2457615.000	MARS		ORBIT DEPARTURE		7.280
	2	2457775.000	EARTH		ORBIT CAPTURE		6.868
						TOTAL DV(KPS)=	14.148

IMP POINTS:	NO.	DATE	DAYS	X(AU)	Y(AU)	Z(AU)	R(AU)
	1	2016 AUG 14	.0	.4414	-1.3495	-.0393	1.4204
	2	2017 JAN 21	160.0	-.5026	.8461	-.0001	.9841

AUX DATA:	NO.	VHP(KPS)	DEC(DEG)	RA(DEG)	PHAZ(DEG)	SET(DEG)	RC(AU)
	1*	10.872	-2.059	227.982	152.742	102.827	.7960
	2*	12.975	.881	125.336	19.101	.000	.0000

* = BODY EQUATORIAL VHP COORDINATES

MASS DATA:	STAGE	DV(KPS)	MR(KG)	MP(KG)	MPMAX(KG)	
	1	7.280	107627.	96752.	99999.	MOMAX(KG)=172300.
	2	6.868	39658.	34962.	99999.	MO(KG)=172300.
						PAYLOAD(KG)= 25015.

RUN DATA:	NO.	TYM GRAD	POSXGRAD	POSYGRAD	POSZGRAD
	1	.000E+00	.000E+00	.000E+00	.000E+00
	2	.000E+00	.000E+00	.000E+00	.000E+00

NS= 1 0 0 1 1 1

NRI= 0